

---

*Supplementary Material*

# Optimization and Engineering of a Self-Sufficient CYP102 Enzyme from *Bacillus amyloliquefaciens* towards Synthesis of In-Chain Hydroxy Fatty Acids

Li Zong <sup>1,2</sup>, Yan Zhang <sup>2</sup>, Zhengkang Shao <sup>1</sup>, Yingwu Wang <sup>1</sup>, Zheng Guo <sup>2</sup>, Renjun Gao <sup>1,\*</sup> and Bekir Engin Eser <sup>2,\*</sup>

<sup>1</sup> Key Laboratory for Molecular Enzymology and Engineering, The Ministry of Education, School of Life Science, Jilin University, Changchun 130021, China; zongli18@mails.jlu.edu.cn (L.Z.); shaozk18@mails.jlu.edu.cn (Z.S.); wyw@jlu.edu.cn (Y.W.)

<sup>2</sup> Department of Biological and Chemical Engineering, Faculty of Technical Sciences, Aarhus University, Gustav Wieds Vej 10, 8000 Aarhus, Denmark; yanhang@bce.au.dk (Y.Z.); guo@bce.au.dk (Z.G.)

\* Correspondence: gaorj@jlu.edu.cn (R.G.), bekireser@bce.au.dk (B.E.E.)

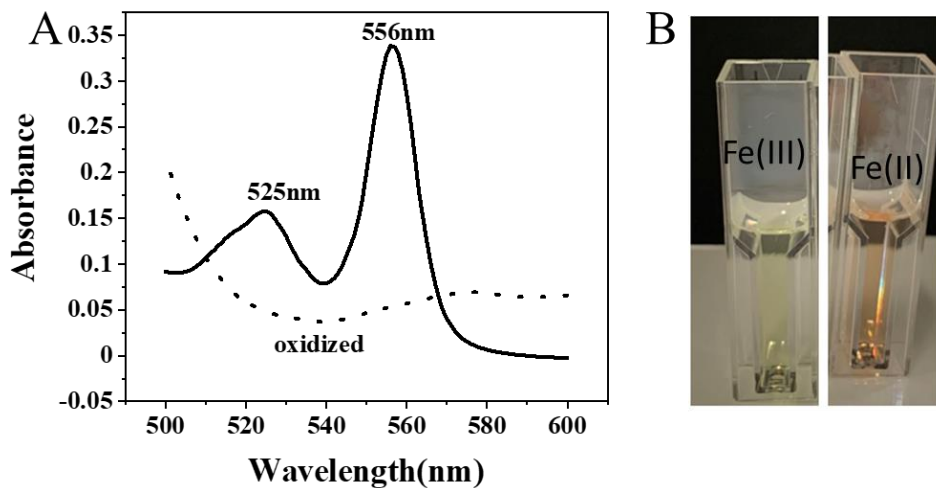


**Figure S1.** Pyridine hemochrome difference spectrum of BAMF2522 (A). Spectra are shown for the oxidized (dotted line) and reduced (solid line) forms. Oxidized sample in yellow color and reduced sample in a reddish color (B).

**Table S1.** Primers used for site-directed mutagenesis of BAMF2522.

Target sites	Oligonucleotide sequences
I266F	F: 5'CTATCAAATCATTACCTTTGTTGCAGGGCATGAAACCACAAGCG 3'
	R: 5'CGCTTGTGGTTCATGCCCGCAAACAAAAGGTAATGATTGATAG 3'
N72S	F: 5' GAAAAGCGATTGATAAAAGCCTCAGCAAAGCCTTGCTG 3'
	R: 5' CAGCAAGGCTTGCTGAGGCTTTATCAAATCGCTTTTC 3'
M187T	F: 5' GCTGCAGGAGGAACCCGCCAATCACAGAG 3'
	R: 5' CTCTGTGATTGGCGGGTTGCCTCCTGCAGC 3'
V218A	F: 5' GTGATGAATGAACTCGGGACCGGATTATTGCTG 3'
	R: 5' CAGCAATAATCCGGTCCGCGAGTTATTCAAC 3'
M240L	F: 5' GACCTTTAGCATTGCTGCTGAAGCGAAAG 3'
	R: 5' CTTTCGCTCAAGCAGCAATGCTAAAAGGTC 3'
S47R	F: 5' GAGACGAAGACCCGACACGGCTCGGAAATTCAAAACG 3'
	R: 5' CGTTTGAAATTCCGAGCCGTGTCGGGTCTCGTCTC 3'
F51Y	F: 5' CGCGGCCTGAGACATAGACCCGACACCG 3'
	R: 5' CGTGTGGGGTCTATGTCTCAGGCCGCG 3'
F89V	F: 5' GAGTCCAGCTCGTAACTAGTCCGTACCGCC 3'
	R: 5' GGCGGTGACGGACTAGTTACGAGCTGGACTCC 3'
F89I	F: 5' GCGGTGACGGACTAATTACGAGCTGGAC 3'
	R: 5' GTCCAGCTCGTAATTAGTCCGTACCGC 3'
A331V	F: 5' GCTGTATCCGACTGTGCCGGCATTTCCCTG 3'
	R: 5' CAGGGAAAATGCCGGCACAGTCGGATACAGC 3'

**Table S2.** Numerical data for temperature dependence experiments.

Temperature (°C)	10	15	20	25	30	35	40	45	50	60	70
Relative activity (%)	49.3±0.3	57.0±0.4	80.1±0.2	77.2±0.0	100.0±1.0	62.8±0.5	68.7±0.1	66.5±0.6	66.1±0.2	48.3±0.6	3.7±0.1

**Table S3.** Numerical data for pH dependence experiments.

Buffer	Acetate–Acetic Acid				
pH	5.0	5.5			
Relative ac- tivity (%)	2.1 ± 0.1	2.4 ± 0.0			
Buffer	Na <sub>2</sub> HPO <sub>4</sub> –NaH <sub>2</sub> PO <sub>4</sub>				
pH	6.0	6.5	7.0	7.5	8
Relative ac- tivity (%)	18.1 ± 0.3	58.1 ± 0.2	65.3 ± 0.0	68.5 ± 0.6	68.9 ± 0.4
Buffer	Tris-HCl				
pH	7.1	7.5	8.0	8.5	8.9
Relative ac- tivity (%)	72.6 ± 0.0	92.0 ± 0.3	76.6 ± 0.2	60.3 ± 0.5	25.9 ± 0.7
Buffer	Glycine-NaOH				
pH	8.6	9.5	10.0	10.6	
Relative ac- tivity (%)	41.8 ± 0.3	9.8 ± 0.2	7.4 ± 0.2	4.7 ± 0.2	
Buffer	MOPS				
pH	6.5	7.0	7.5	8.0	
Relative ac- tivity (%)	15.3 ± 0.1	84.7 ± 1.4	86.9 ± 0.7	78.6 ± 0.8	
Buffer	HEPES				
pH	7	7.6	8.0		
Relative ac- tivity (%)	100 ± 0.6	95.5 ± 1.3	71.9 ± 0.0		

**Table S4.** Numerical data for thermostability measurements.

Temperature (°C)	4	20	30	40	50	60	70
Relative activity (%)	92.0 ± 0.3	96.9 ± 0.4	98.6 ± 0.1	100.0 ± 1.0	0	0	0

**Table S5.** Total conversion levels and regioselectivity data for the hydroxylation of different substrates by wild-type and rational design mutants of BAMF2522. The data were analyzed by GC-MS.

Mutation codes of multi-site mutants with respect to the wild type BAMF2522:

R31: A331V/ F89I/ N72S/M187T

R41: A331V/ F89I/ N72S/M187T/ V218A/M240L

RY5: A331V/F89I/ S49R/F53Y

C12:0		Product distribution (%)
-------	--	--------------------------

	Conversion	$\omega$ -5	$\omega$ -4	$\omega$ -3	$\omega$ -2	$\omega$ -1
WTBA2522	9.8±0.1	1.3 ± 0.5	1.7 ± 0.6	40 ± 5	40 ± 5	17 ± 1
F89V	4.9±0.7	12 ± 1	8.3 ± 0.3	49 ± 1	21 ± 0	9 ± 1
F89I	0.4± 0.2	-	-	50 ± 3	22 ± 7	29 ± 4
I266F	1.1± 0.0	-	-	19 ± 6	49 ± 3	32 ± 9
A331V	6.0±0.5	-	1.8 ± 0.1	29 ± 1	39 ± 1	30 ± 1
R31	3.0±0.4	8 ± 2	18 ± 0	22 ± 3	40 ± 10	12 ± 5
R41	1.6± 0.1	18 ± 4	19 ± 1	36 ± 3	13 ± 2	13 ± 3
RY5	1.2±0.2	10 ± 1	14 ± 7	34 ± 1	15 ± 1	27 ± 6
F89I/ A331V	4.1± 0.0	7 ± 1	13 ± 2	36 ± 1	18 ± 1	27 ± 1

C14:0	Product distribution (%)							
	Conversion(%)	$\omega$ -7	$\omega$ -6	$\omega$ -5	$\omega$ -4	$\omega$ -3	$\omega$ -2	$\omega$ -1
WTBA2522	28.2 ± 0.4	1.7 ± 0.2	0.5 ± 0.3	2.1 ± 0.6	9 ± 1	46 ± 1	32.8 ± 0.1	8.3 ± 0.5
F89V	28.6±6.8	35 ± 1	10 ± 1	19 ± 2	15 ± 2	12 ± 1	7 ± 1	3 ± 1
F89I	2.6±0.2	16 ± 3	12 ± 2	35 ± 4	13 ± 2	13 ± 4	6 ± 2	6.2 ± 0.2
I266F	7.1±0.4	-	-	2.9 ± 0.6	3.5 ± 0.9	24 ± 3	53 ± 1	17 ± 3.0
A331V	3.5±0.8	-	-	6.3 ± 3.7	10 ± 0	36 ± 0	22 ± 2	26 ± 1
A331V/F89I	19.3±4.1	17 ± 0	6 ± 1	29 ± 3	20 ± 1	10 ± 3	4.4 ± 1.5	13 ± 1
R31	5.7±0.4	32 ± 8	12 ± 1	26 ± 2	20 ± 5	11 ± 3	<1.0	<1.0
R41	8.7± 1.2	36 ± 2	10 ± 4	30 ± 4	17 ± 2	8 ± 1	<1.0	<1.0
RY5	4.2±2.9	12 ± 2	7 ± 0	28 ± 5	15 ± 3	14 ± 3	9 ± 1	16 ± 1

C15:0 <sup>1</sup>	Product distribution (%)								
	Conversion (%)	$\omega$ -8	$\omega$ -7	$\omega$ -6	$\omega$ -5	$\omega$ -4	$\omega$ -3	$\omega$ -2	$\omega$ -1
WTBA2522	53	-	9 <sup>2</sup>		2	6	19	61	3
F89V	67	3	12 ± 4		<2	<2	3	80	<2
F89I	39	5	9		2	<2	4	76	<2
A331V	35	-	6		3	2	7	76	6
R31	41	5	3		<2	<1	<1	89	<1
RY5	39	7	6		2	2	4	73	6
R41	61	5	9		<1	<1	<2	81	<1
I266F	40	-	9		<2	<1	2	84	3
A331V/F89I	48	6	13 ± 4		3	3	3	65	7

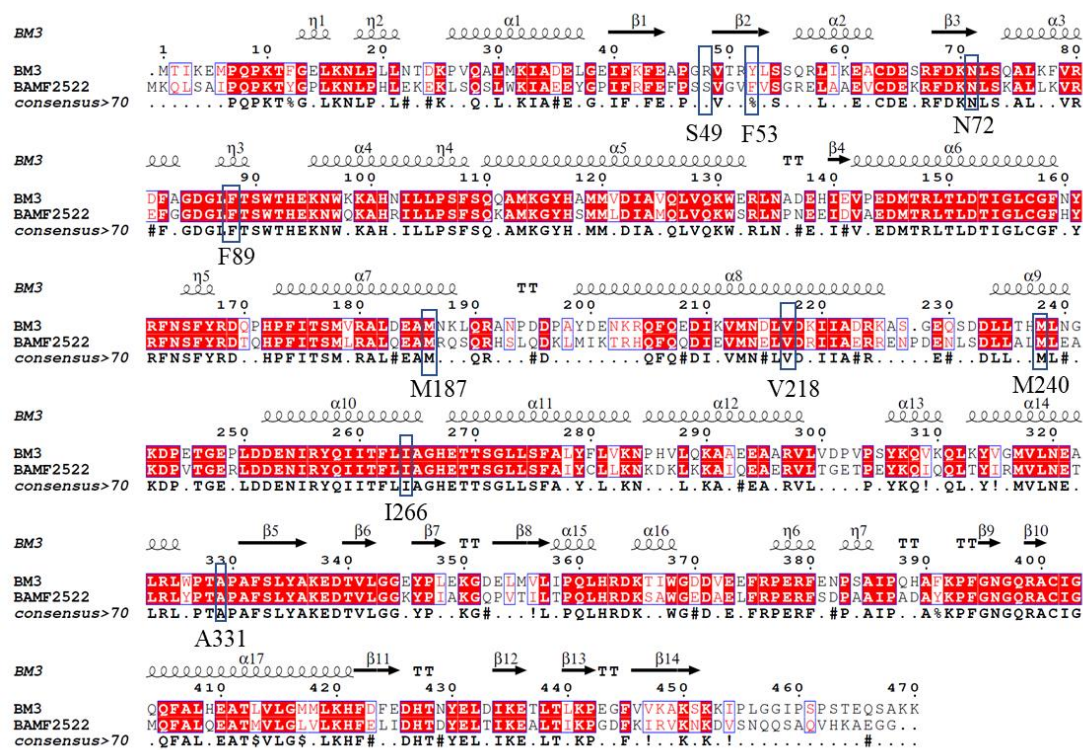
<sup>1</sup>Due to the overlap of an impurity peak (observed only with whole cell assays) with  $\omega$ -2 peak, the percentages reported here for C15:0 are broad estimates. Thus,  $\omega$ -2 ratio is most probably overestimated due to ambiguity of peak areas, leading to lower ratios than actual values for other products.

<sup>2</sup>In our earlier study,  $\omega$ -7 product had not been detected for the wild-type enzyme (Ref. 36 in the main text). In this study,  $\omega$ -7 product has also been detected eluting together with  $\omega$ -6 product (**Fig. S7**).

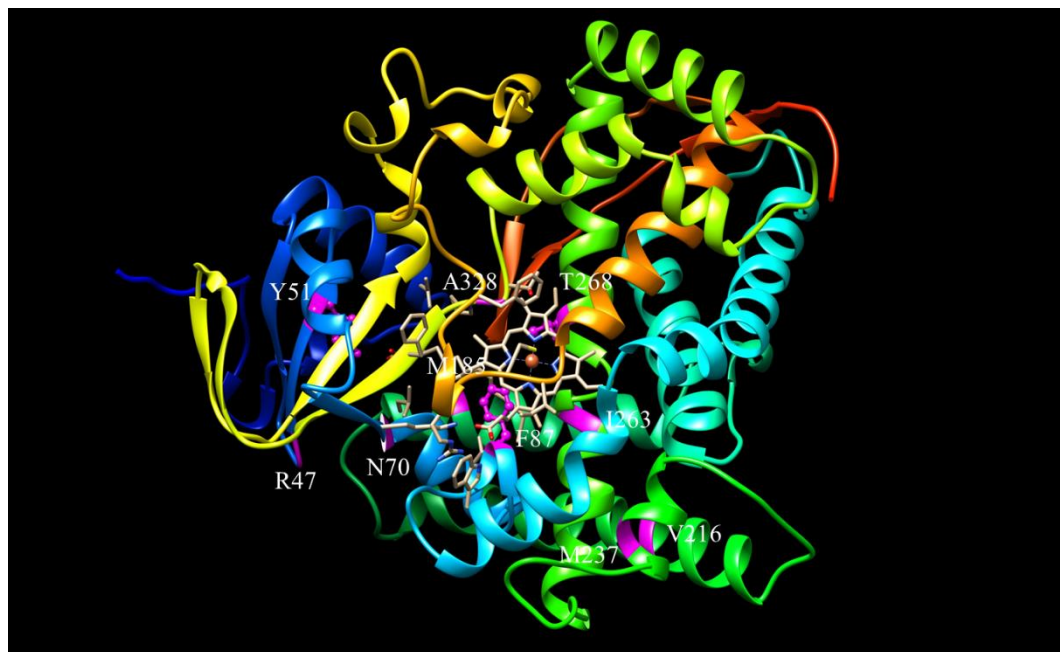
C16:0	Product distribution (%)									
	Conversion (%)	ω-9	ω-8	ω-7	ω-6	ω-5	ω-4	ω-3	ω-2	ω-1
WTBAMF2522	14.2 ± 0.6	-	-	20.2 ± 3.2	9.3 ± 2.5	7.6 ± 1.3	10.0 ± 0.2	19.0 ± 0.8	24.4 ± 0.2	9.5 ± 0.1
F89I	14.0 ± 3.3	70.9 ± 0.4			7.3 ± 0.1	3.0 ± 0.1	2.3 ± 0.0	2.1 ± 0.4	5.1 ± 0.6	9.3 ± 0.9
A331V	28.5 ± 2.2	-	-	24.4 ± 1.1	8.7 ± 1.3	7.2 ± 0.3	3.8 ± 0.4	8.9 ± 0.6	20.0 ± 0.1	26.9 ± 0.4
R31	5.3 ± 1.1	77.1 ± 2.2			7.2 ± 0.7	2.4 ± 0.6	2.1 ± 0.1	1.2 ± 0.1	5.6 ± 0.3	4.5 ± 0.4
R41	7.1 ± 0.7	83.6 ± 0.6			5.7 ± 0.7	2.1 ± 0.5	1.4 ± 0.1	1.3 ± 0.2	1.3 ± 0.2	4.4 ± 0.8
RY5	10.1 ± 1.1	48.3 ± 1.2			6.3 ± 0.2	4.0 ± 0.9	6.0 ± 0.1	6.5 ± 0.6	11.1 ± 1.3	17.8 ± 1.0
I266F	4.6 ± 0.0	-	-	17.5 ± 2.1	9.6 ± 1.2	4.9 ± 0.1	2.4 ± 0.4	3.4 ± 0.2	38.0 ± 0.9	24.2 ± 0.5
A331V/F89I	8.3 ± 0.7	48.8 ± 2.2			5.2 ± 0.8	3.4 ± 0.5	2.4 ± 0.1	2.9 ± 0.2	8.5 ± 0.1	28.9 ± 0.4

C18:0	Product distribution (%)			
	Conversion (%)	ω-3	ω-2	ω-1
WTBA2522	5.5 ± 0.5	24 ± 6	50 ± 2	26 ± 5
F89I	-	-	-	-
F89V	-	-	-	-
A331V	5.3 ± 0.4	23 ± 0	29 ± 4	48 ± 3
A331V/F89I	-	-	-	-
R31	-	-	-	-
R41	-	-	-	-
RY5	2.0 ± 0.5	52 ± 7	22 ± 7	26 ± 0
I266F	-	-	-	-

C20:0	Product distribution (%)					
	Conversion (%)	ω-5	ω-4	ω-3	ω-2	ω-1
WTBA2522	2.7 ± 0.4	--		52 ± 0	37 ± 1	11 ± 1
F89I	-	-	-	-	-	-
F89V	-	-	-	-	-	-
A331V	8.1 ± 1.5	9 ± 3	11 ± 1	21 ± 1	27 ± 1	31 ± 2
R31	-	-	-	-	-	-
R41	-	-	-	-	-	-
RY5	-	-	-	-	-	-
F89I/A328V	-	-	-	-	-	-
I266F	-	-	-	-	-	-



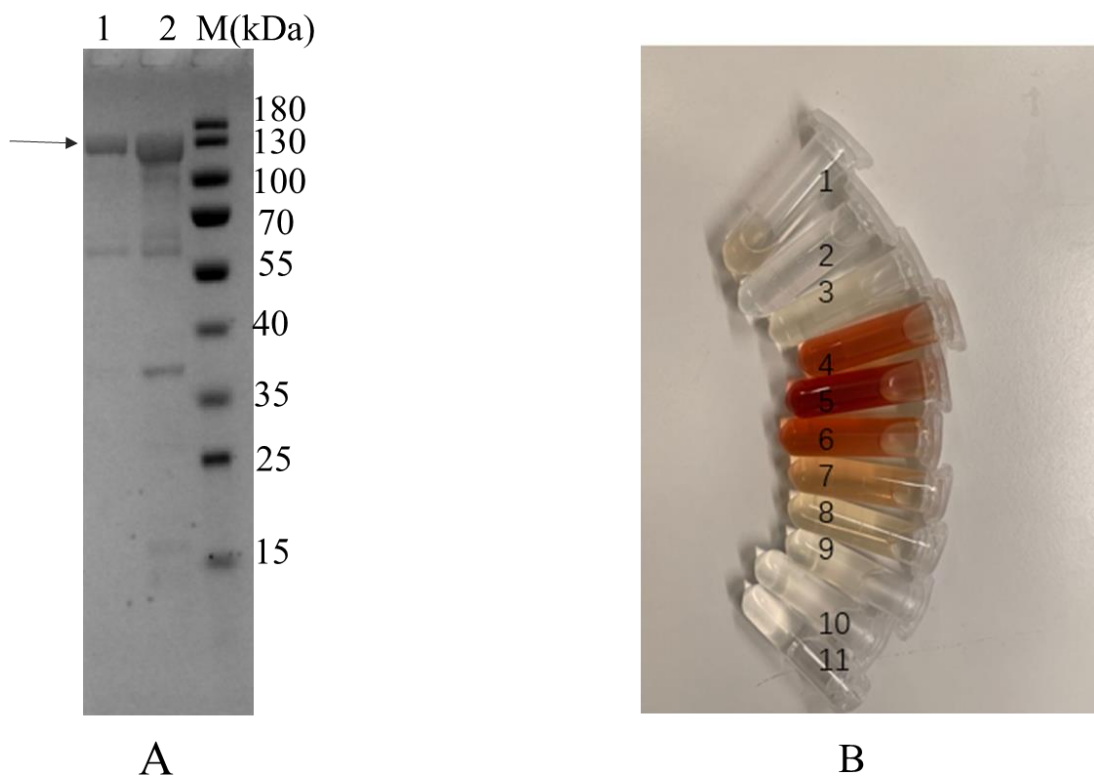
**Figure S2.** Sequence alignment of BM3 and BAMF2522. The mutation positions are highlighted. Sequence alignments were performed by ClustalW; BM3 structure (PDB:1FAG) was used to display the secondary structure and ENDscript website was used for plotting the sequence alignment results (Robert, X. and P. Gouet, Deciphering key features in protein structures with the new ENDscript server. Nucleic Acids Res, 2014. 42(Web Server issue): p. W320-4).



**Figure S3.** Structure of wild-type BM3 (pdb id: 1FAG). The residue positions corresponding to mutations performed on BAMF2522 in this study are indicated in magenta color (Table S9). Iron is shown in orange. The residue numbering is according to BM3 sequence.

**Table S6.** Comparison of the mutated residue positions in the protein sequences of BM3 and BAMF2522.

BM3	BAMF2522
R47	S49
Y51	F53
N70S	N72
F87	F89
M185	M187
V216	V218
M237	M240
I263	I266
A328	A331

**Figure S4.** SDS-PAGE analysis the purified BAMF2522 (A), and the color of the protein elution fractions in the collection tube (B). In (A), lane M is protein marker, lane 1 is purified BAMF2522.

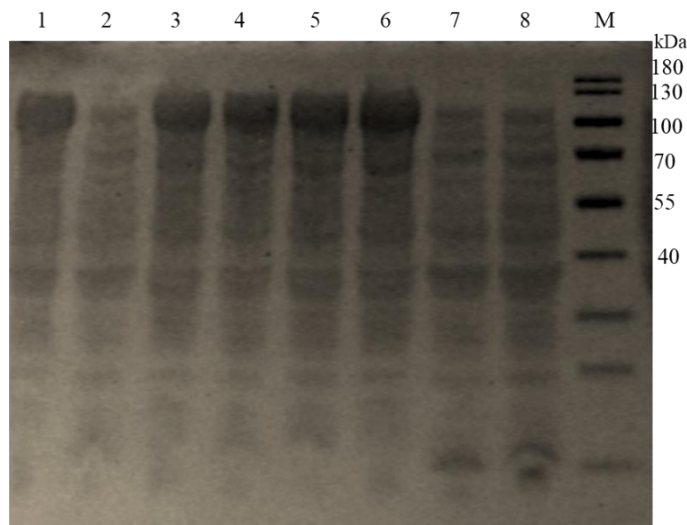
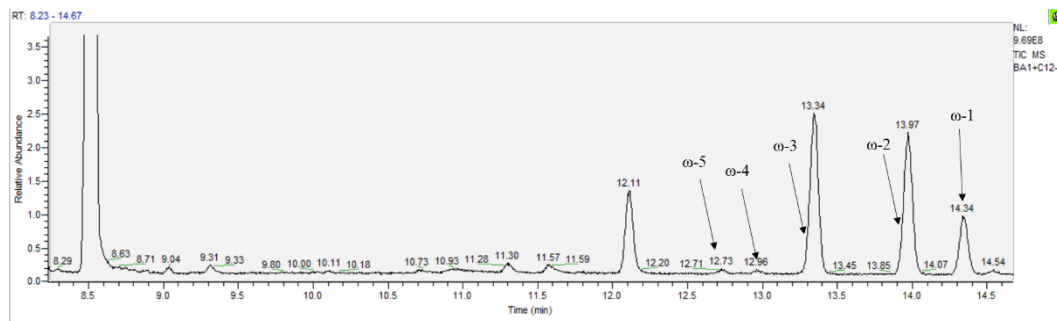


**Figure S5.** SDS-PAGE analysis the whole cell protein expression. Lane M: protein marker, Lane1: BAMF2522, Lane2: RY5, Lane3: BAMF2522 I266F, Lane4: BAMF2522 A331V, Lane5: BAMF2522 A331V/F89I, Lane6: BAMF2522 F89I, Lane7: R31, Lane8: R41.

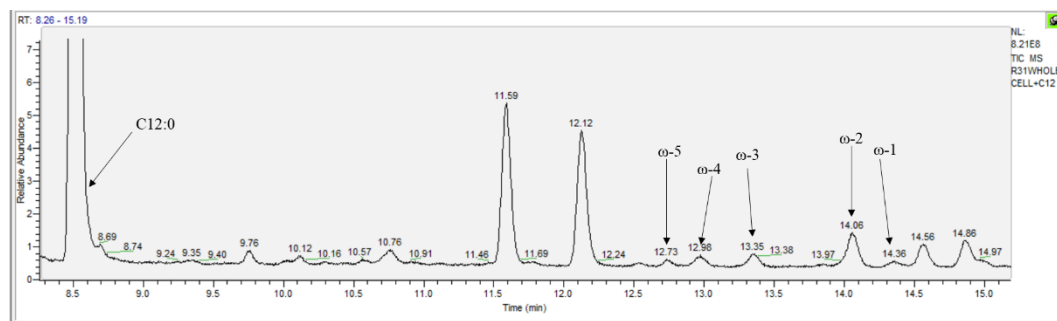
**Figure S6.** Typical GC-MS analysis chromatograms of the derivatized whole-cell oxidation turnovers of BAMF2522 and some variants with dodecanoic, tetradecanoic, pentadecanoic, palmitic, octadecanoic, arachidic and oleic acids.

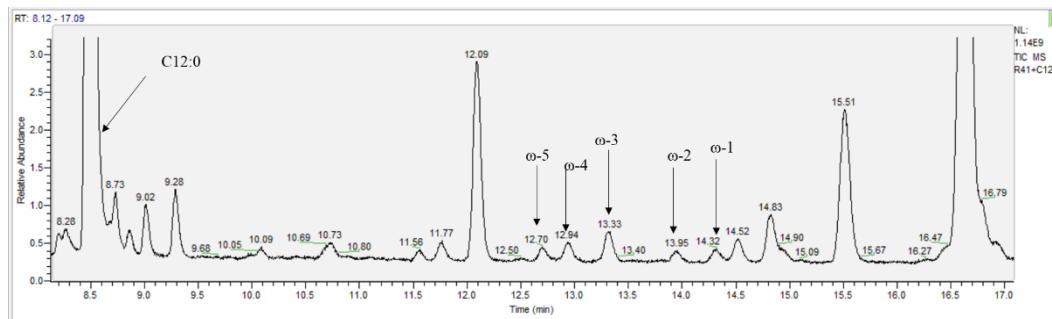
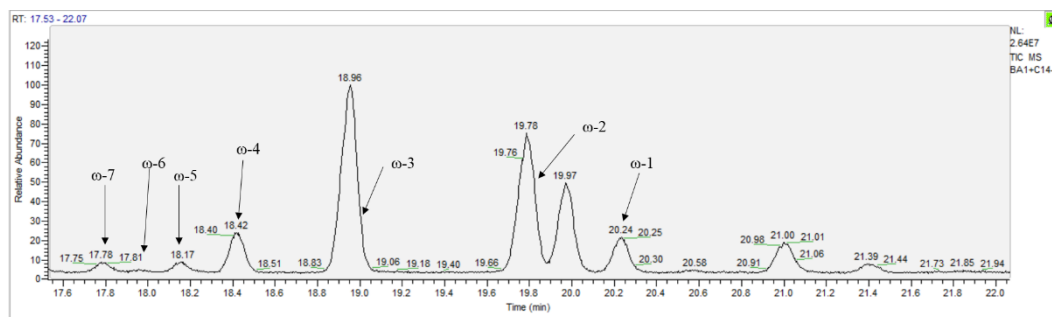
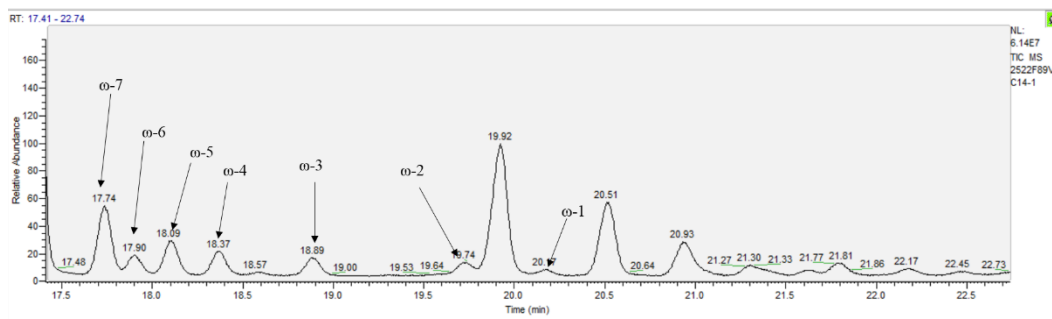
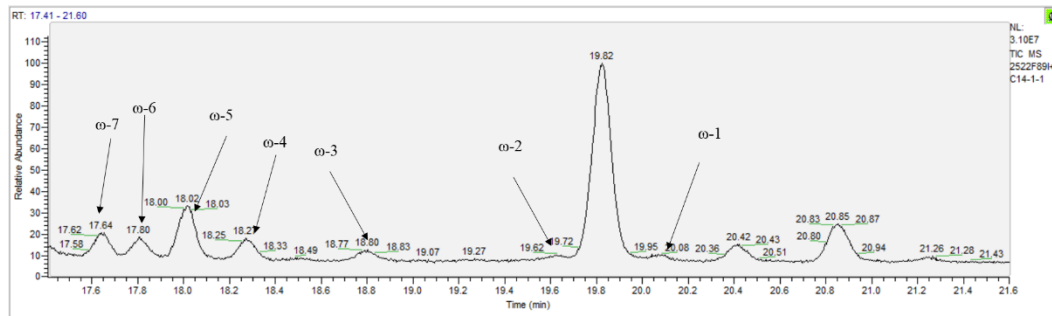
#### A: Dodecanoic acid (C12:0)

a: C12:0 + WT BAMF 2522

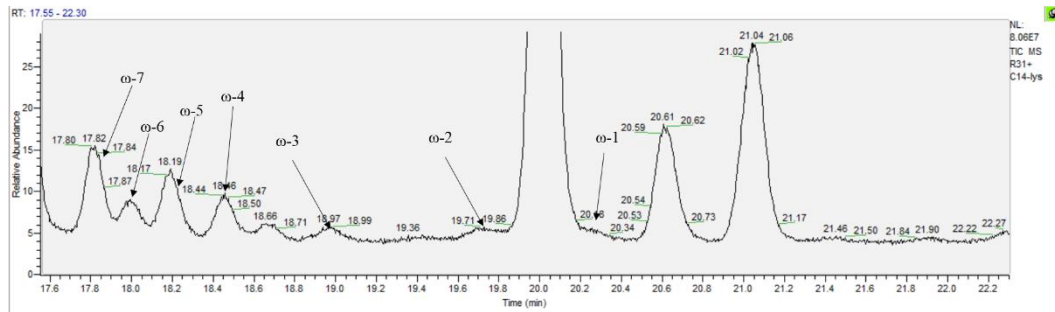


b: C12:0 + BAMF 2522 R31

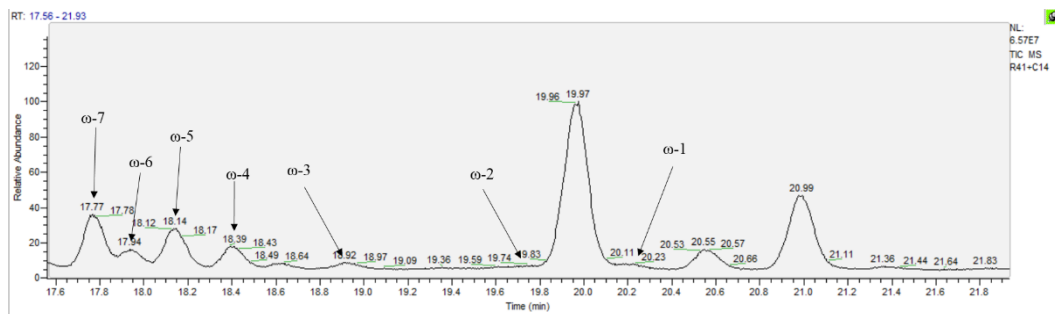


**c: C12:0 + BAMF2522 R41****B: Tetradecanoic acid (C14:0)****a: C14:0 + WT BAMF2522****b: C14:0 + BAMF2522 F89V****c: C14:0 + BAMF2522 F89I**

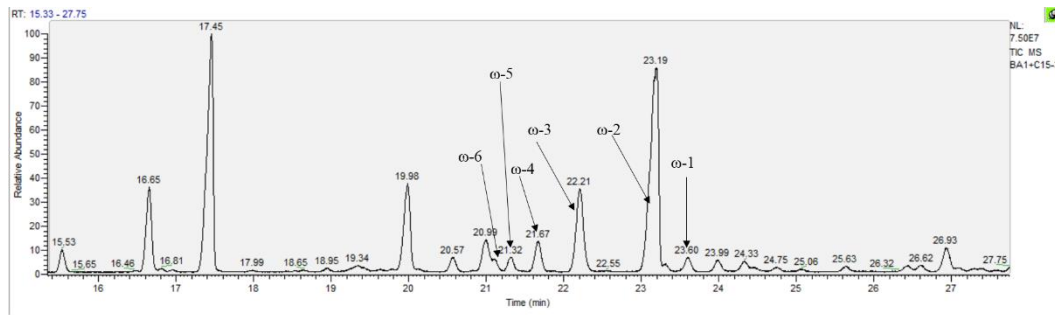
d: C14:0 + BAMF2522 R31



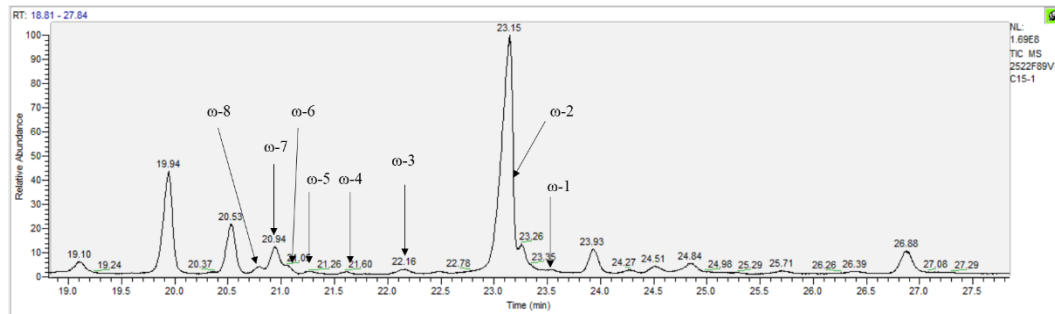
e: C14:0 + BAMF2522 R41

**C: Pentadecanoic acid (C15:0)**

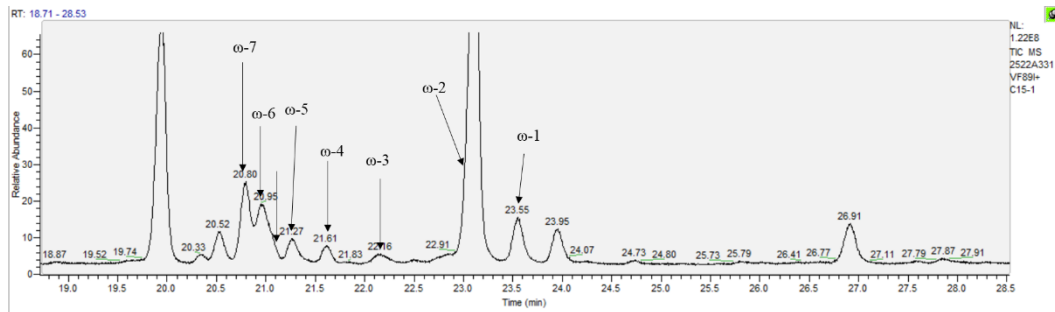
a: C15:0 + WT BAMF2522



b: C15:0+BA2522 F89V

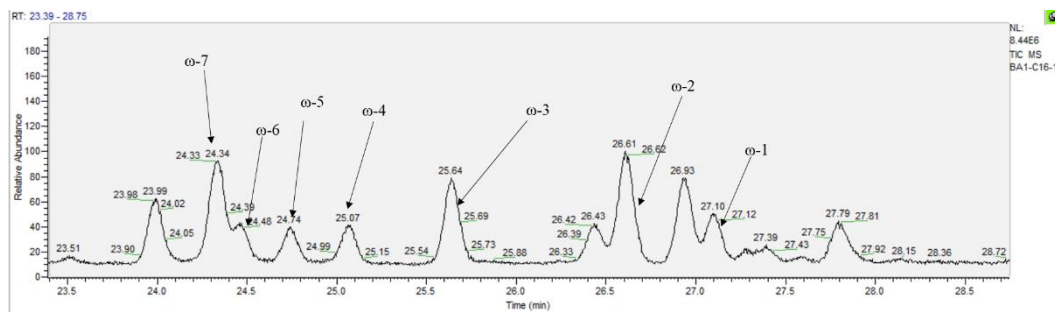


## c: C15:0 + BAMF2522 A331V/F89I

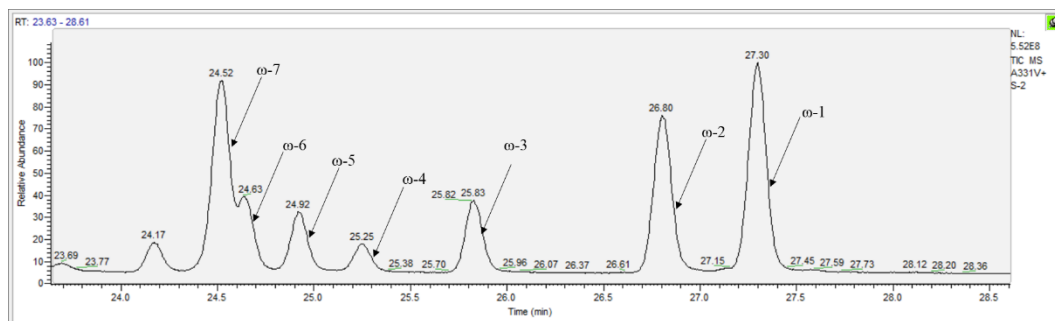
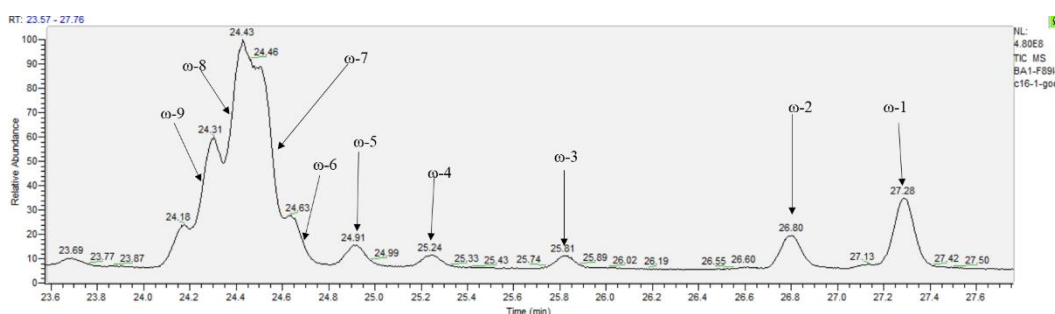


## D: Palmitic acid (C16:0)

## a: C16:0+ WT BAMF2522

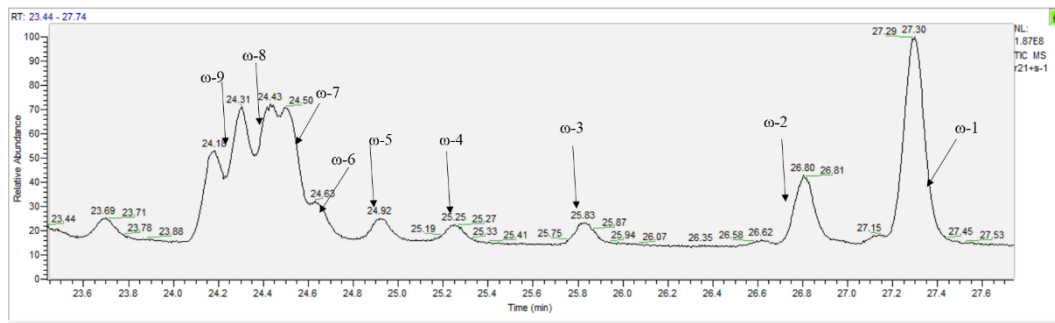


## b: C16:0+BAMF2522 A331V

c: C16:0+BAMF2522 F89I<sup>1</sup>

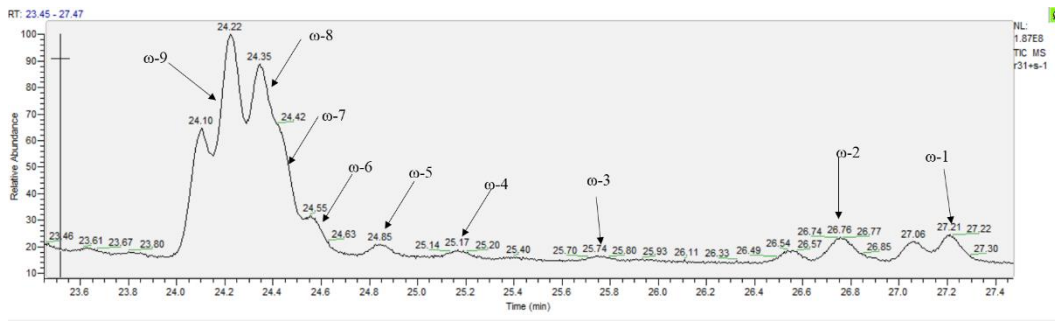
<sup>1</sup>The peak at 24.18 min is a contaminant peak and was not taken into account in calculating the [ $\omega$ -9 +  $\omega$ -8 +  $\omega$ -7] total peak area. For the calculation of peak areas in the case of overlapping peaks, either perpendicular drop method was used or non-overlapping half of the peak was multiplied by 2 (considering symmetric peak shape, as is the case for most peaks), depending on resolution and relative intensities of the peaks.

#### d: C16:0+BAMF2522 F89I/A331V<sup>1</sup>



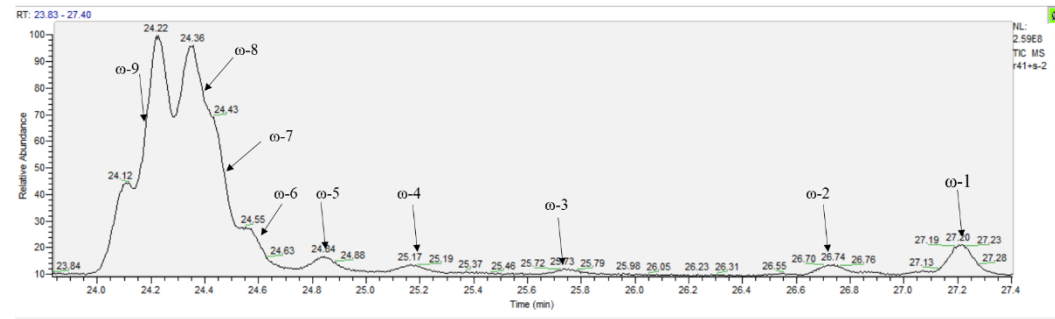
<sup>1</sup>The peak at 24.18 min is a contaminant peak and was not taken into account in calculating the [ $\omega$ -9 +  $\omega$ -8 +  $\omega$ -7] total peak area. For the calculation of peak areas in the case of overlapping peaks, either perpendicular drop method was used or non-overlapping half of the peak was multiplied by 2 (considering symmetric peak shape, as is the case for most peaks), depending on resolution and relative intensities of the peaks.

#### e: C16:0+BAMF2522 R31<sup>1</sup>



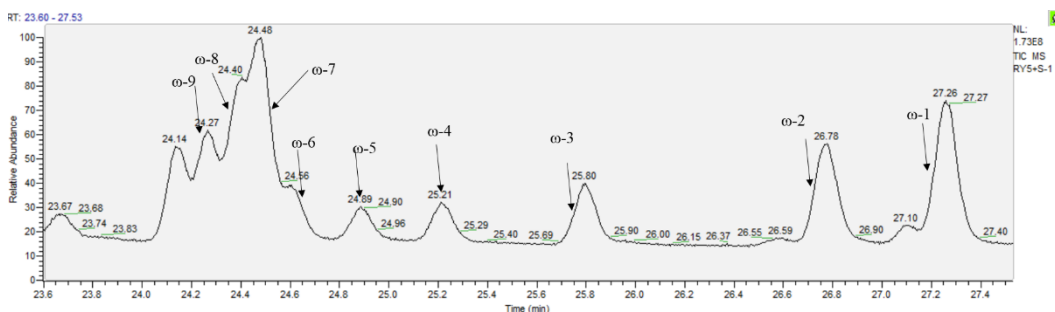
<sup>1</sup>The peak at 24.10 min is a contaminant peak and was not taken into account in calculating the [ $\omega$ -9 +  $\omega$ -8 +  $\omega$ -7] total peak area. For the calculation of peak areas in the case of overlapping peaks, either perpendicular drop method was used or non-overlapping half of the peak was multiplied by 2 (considering symmetric peak shape, as is the case for most peaks), depending on resolution and relative intensities of the peaks.

#### f: C16:0+BAMF2522 R41<sup>1</sup>



<sup>1</sup>The peak at 24.12 min is a contaminant peak and was not taken into account in calculating the [ $\omega$ -9 +  $\omega$ -8 +  $\omega$ -7] total peak area. For the calculation of peak areas in the case of overlapping peaks, either perpendicular drop method was used or non-overlapping half of the peak was multiplied by 2 (considering symmetric peak shape, as is the case for most peaks), depending on resolution and relative intensities of the peaks.

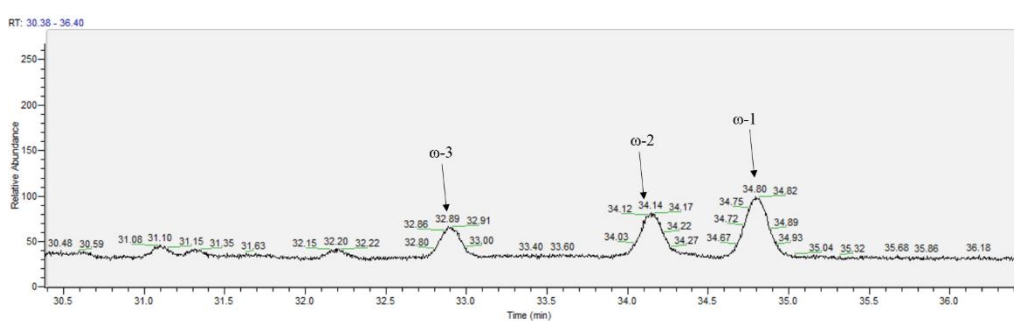
g: C16:0+BAMF2522 RY5<sup>1</sup>



<sup>1</sup>The peak at 24.14 min is a contaminant peak and was not taken into account in calculating the [ $\omega$ -9 +  $\omega$ -8 +  $\omega$ -7] total peak area. For the calculation of peak areas in the case of overlapping peaks, either perpendicular drop method was used or non-overlapping half of the peak was multiplied by 2 (considering symmetric peak shape, as is the case for most peaks), depending on resolution and relative intensities of the peaks.

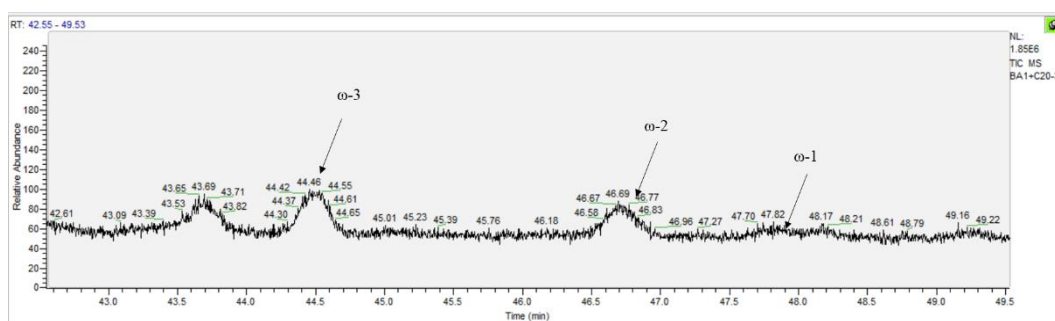
### E: Octadecanoic acid (C18:0)

a: C18:0 + BAMF2522 A331V

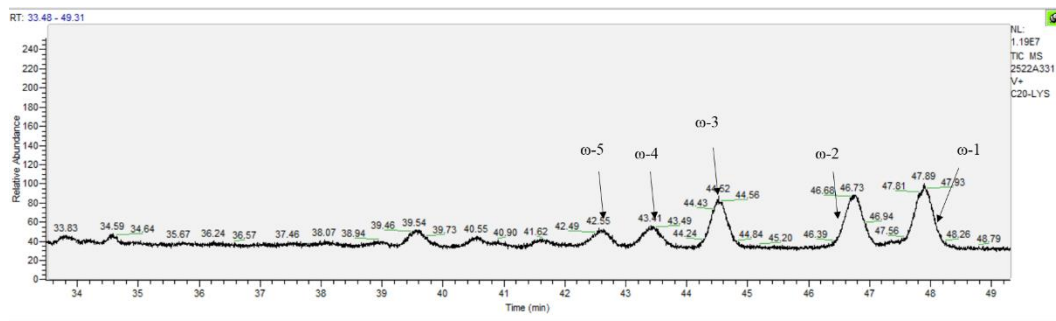


### F: Arachidic acid (C20:0)

a: C20:0 + WT BAMF2522

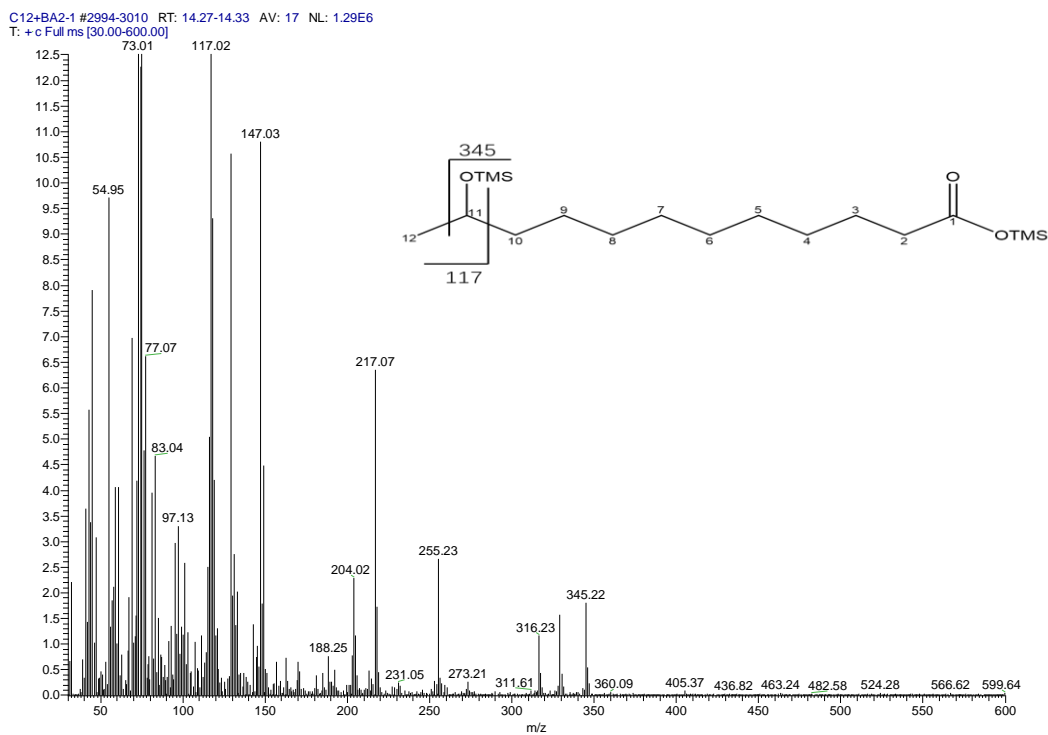


b: C20:0 + BA2522 A331V

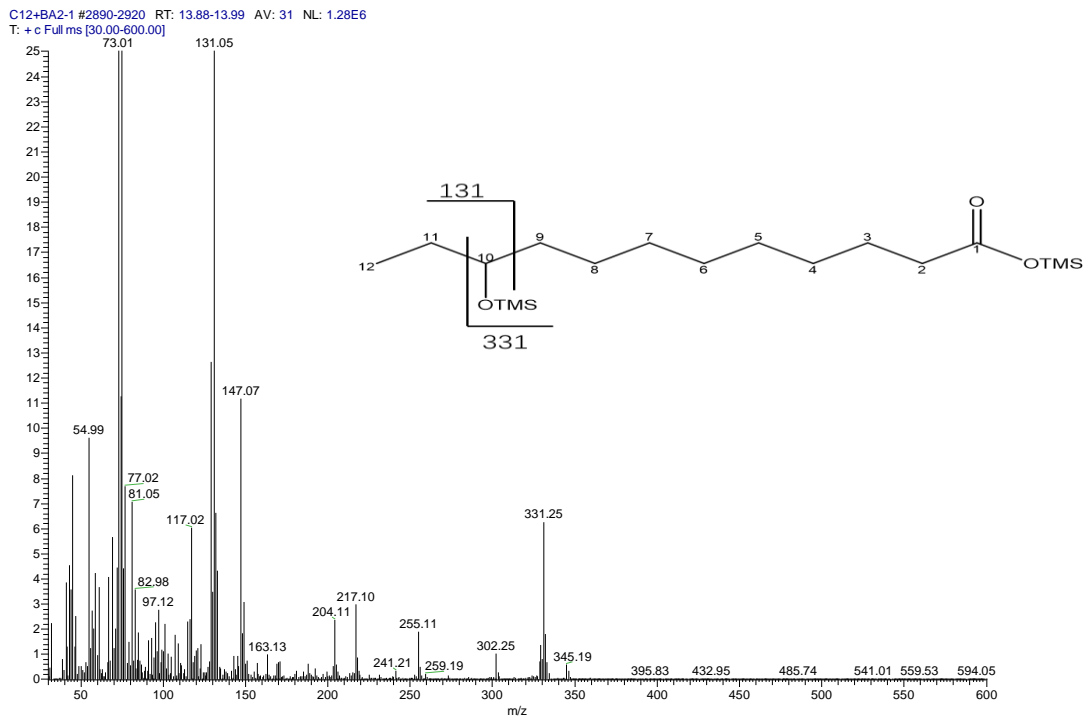
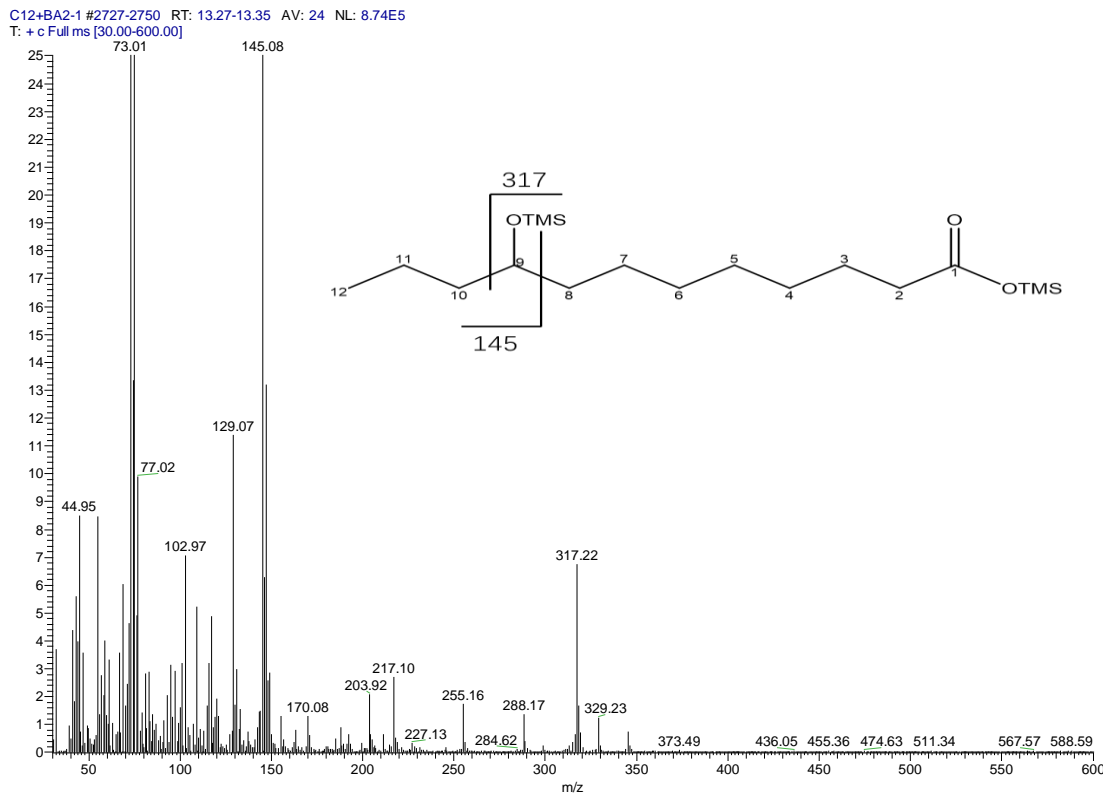


**Figure S7.** Mass spectra and fragmentation patterns for the HFA products obtained from enzymatic transformations in this study.

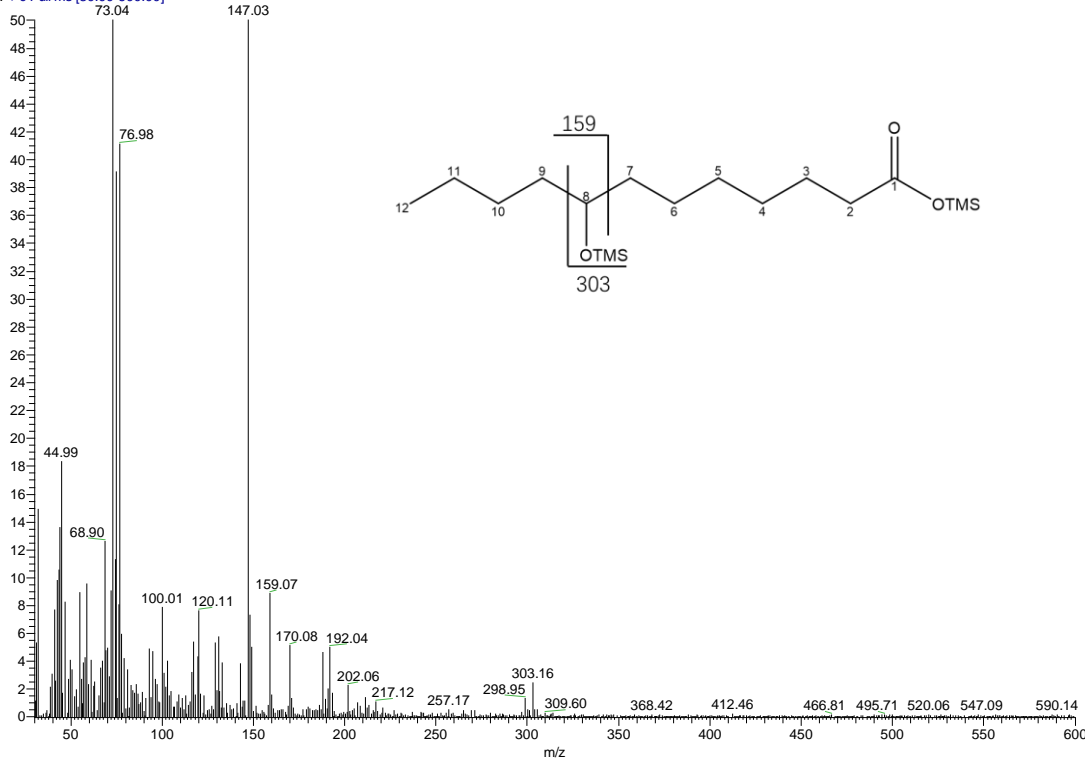
#### Products from Dodecanoic acid (C12:0)



Dodecanoic ω-1 product, RT:14.3 min

Dodecanoic  $\omega$ -2, RT:13.93 minDodecanoic  $\omega$ -3, RT:13.31 min

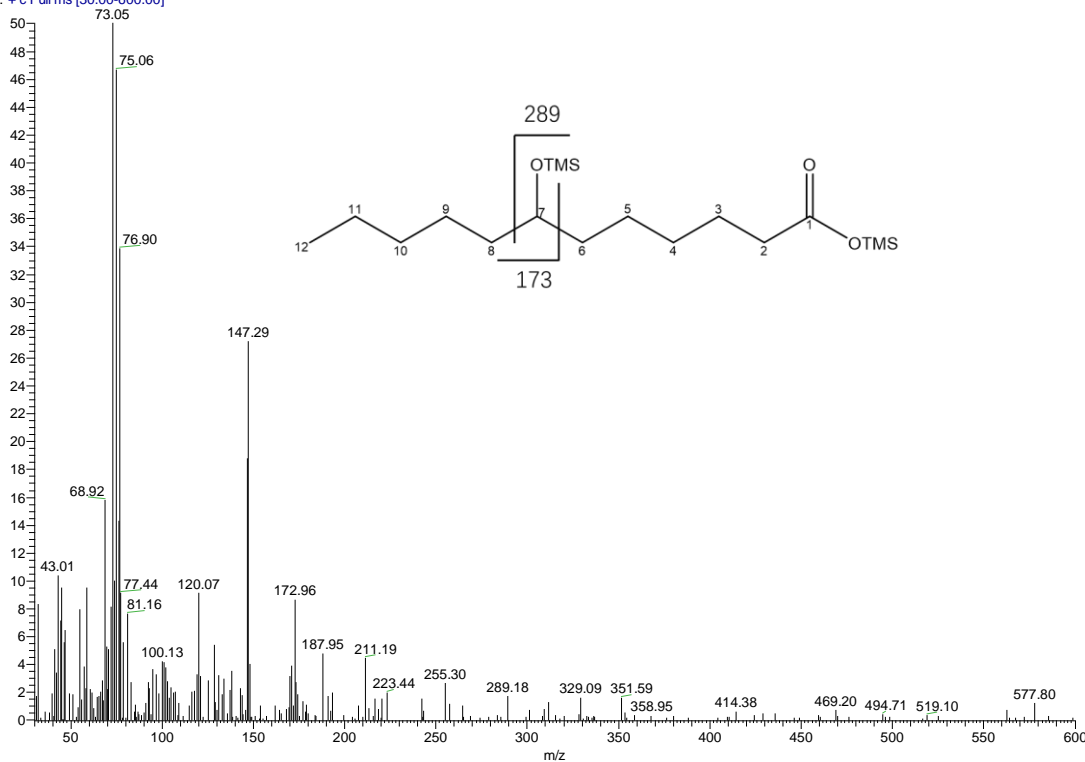
BA1+C12-3 #2640-2659 RT: 12.94-13.01 AV: 20 NL: 1.82E5  
T: + c Full ms [30.00-600.00]



Dodecanoic  $\omega$ -4,

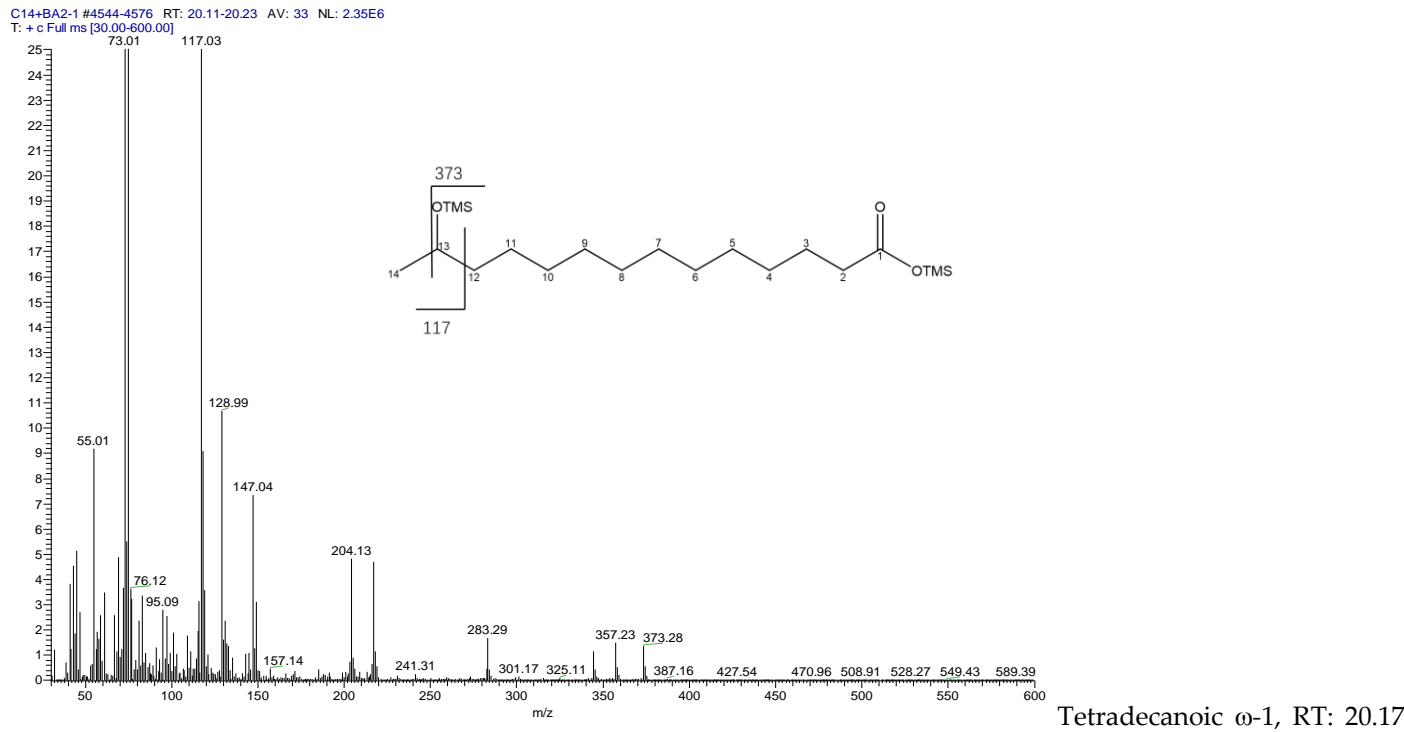
RT:12.96 min

BA1+C12-3 #2588 RT: 12.74 AV: 1 NL: 2.31E5  
T: + c Full ms [30.00-600.00]

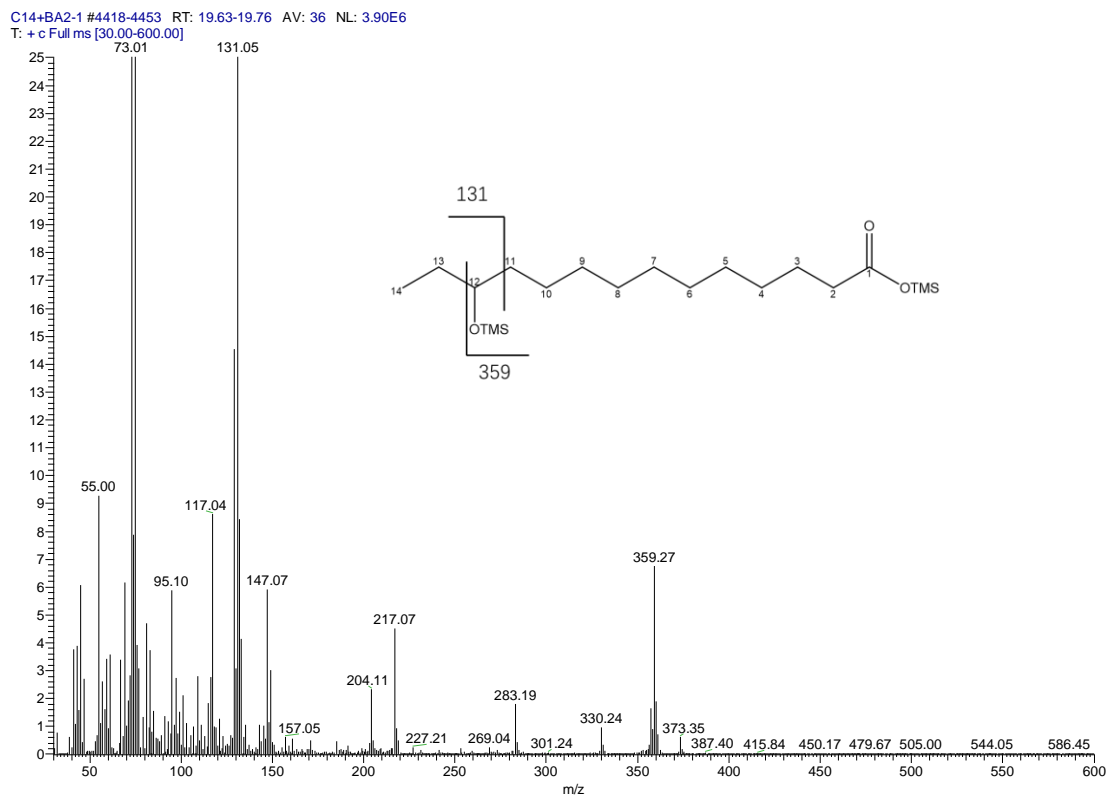


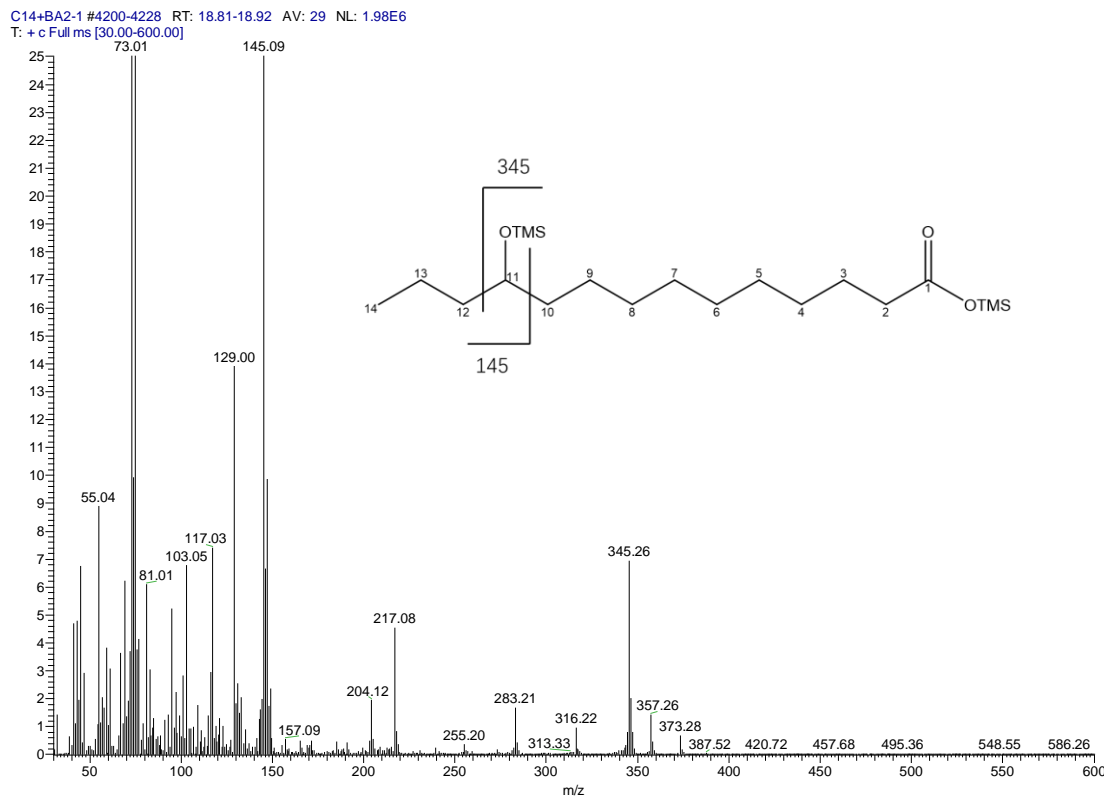
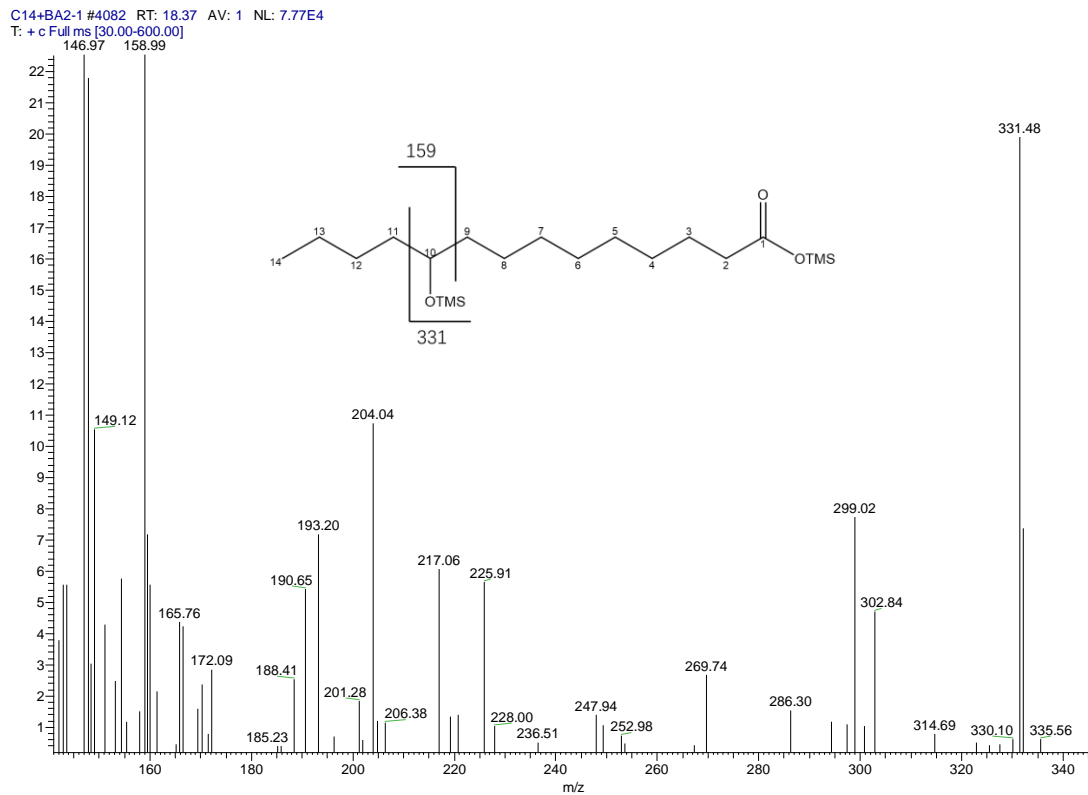
Dodecanoic  $\omega$ -5, RT:12.74 min

### Products from tetradecanoic acid (C14:0)

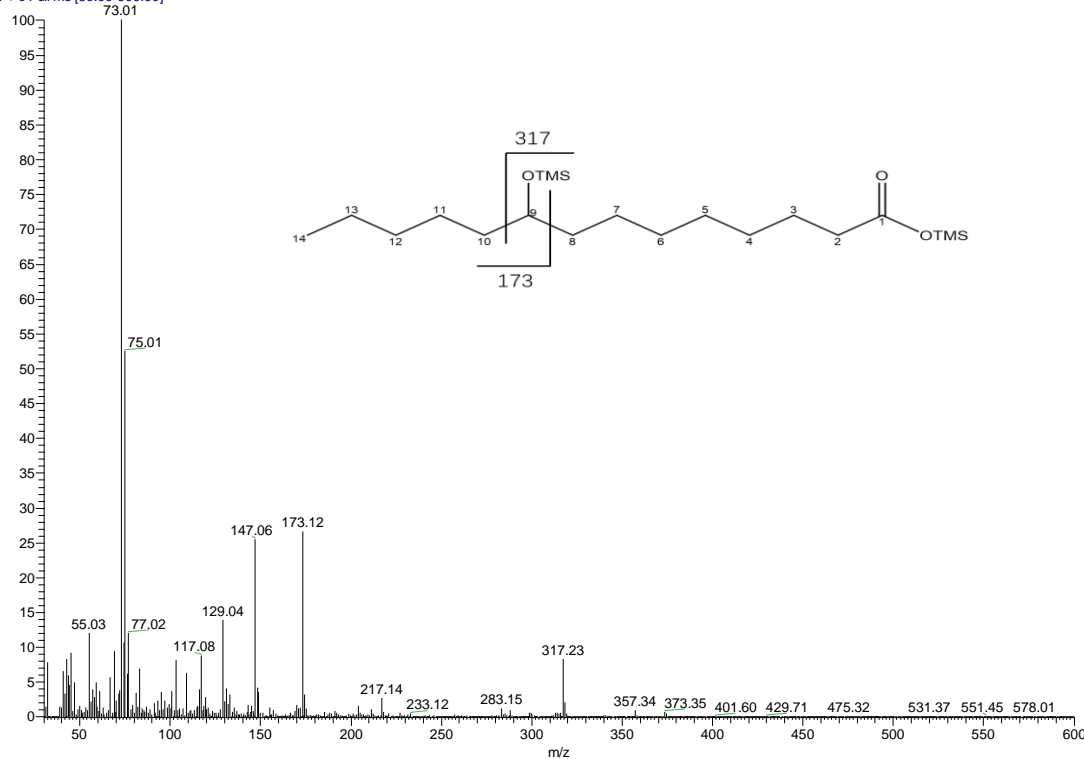


min

Tetradecanoic  $\omega$ -2, RT: 19.73 min

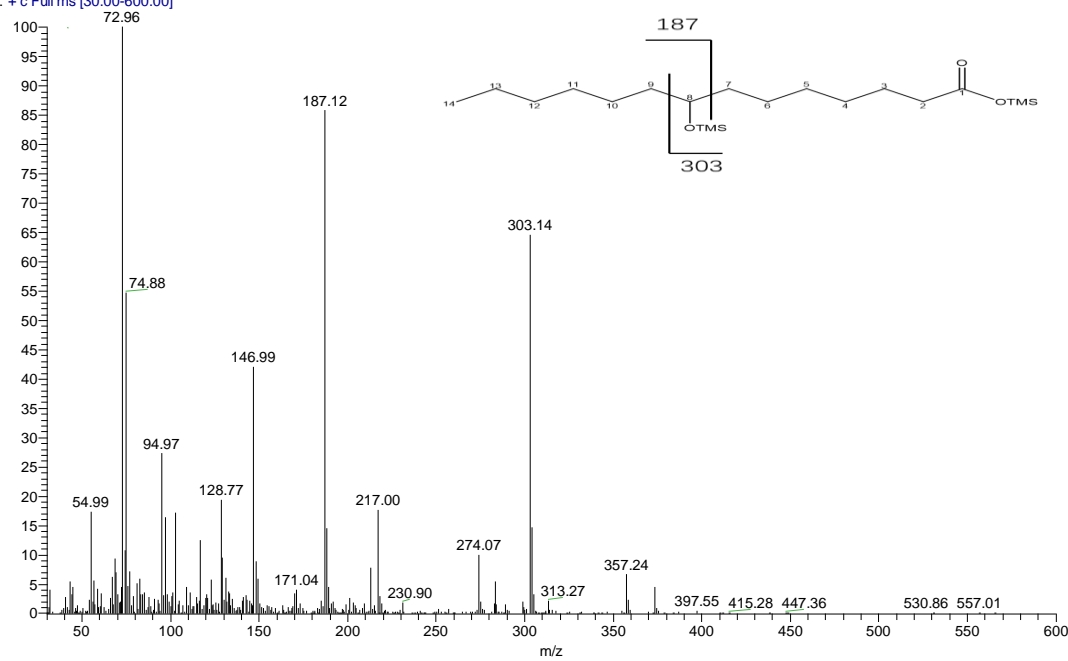
Tetradecanoic  $\omega$ -3, RT: 18.88 minTetradecanoic  $\omega$ -4, RT: 18.36 min

BA1-C14-2 #4011-4039 RT: 18.10-18.21 AV: 29 NL: 3.82E5  
T: + c Full ms [30.00-600.00]

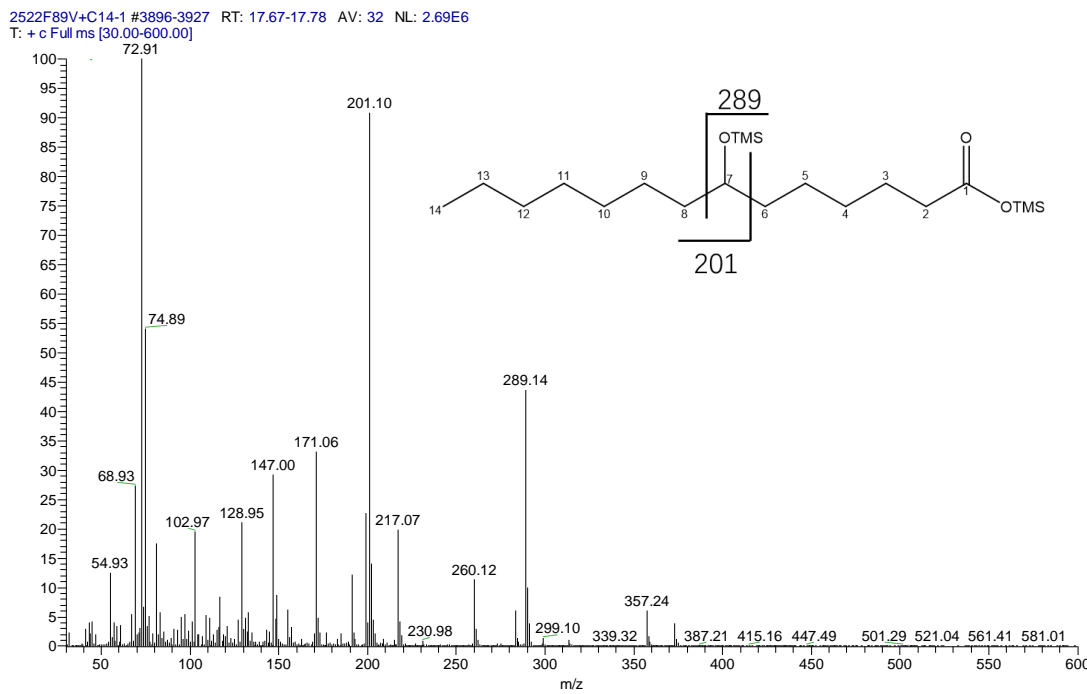


Tetradecanoic  $\omega$ -5, RT:18.17 min

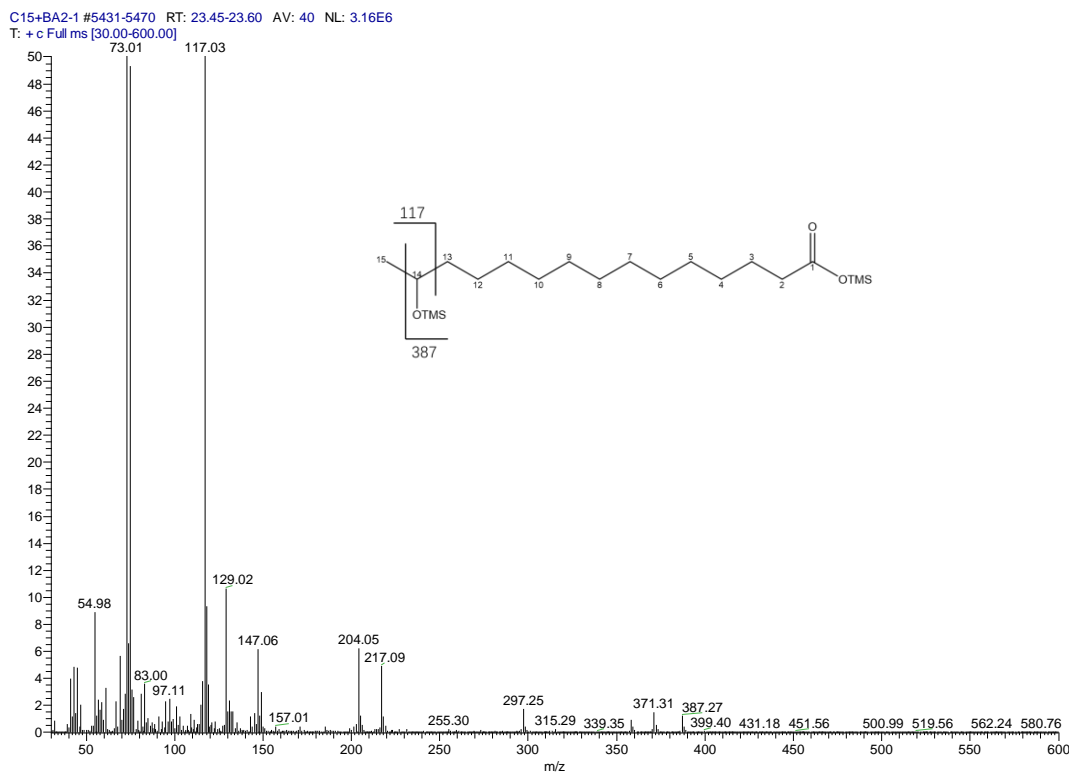
2522F89V+C14-1 #3956 RT: 17.89 AV: 1 NL: 1.24E6  
T: + c Full ms [30.00-600.00]

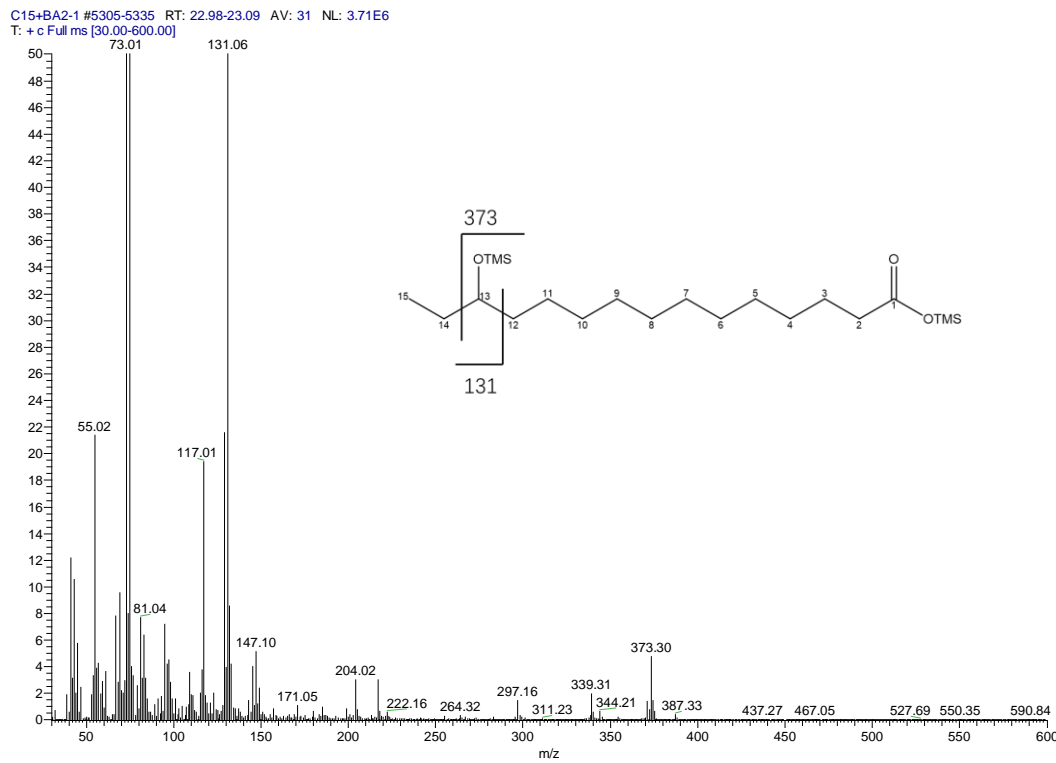
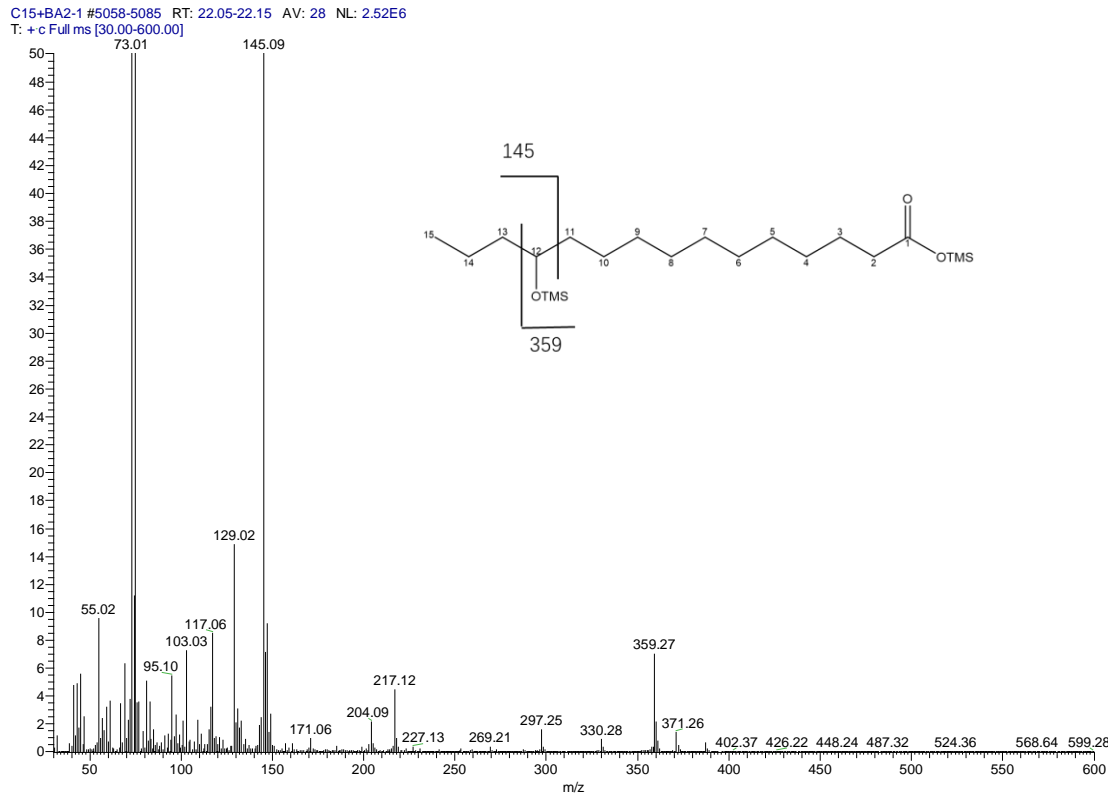


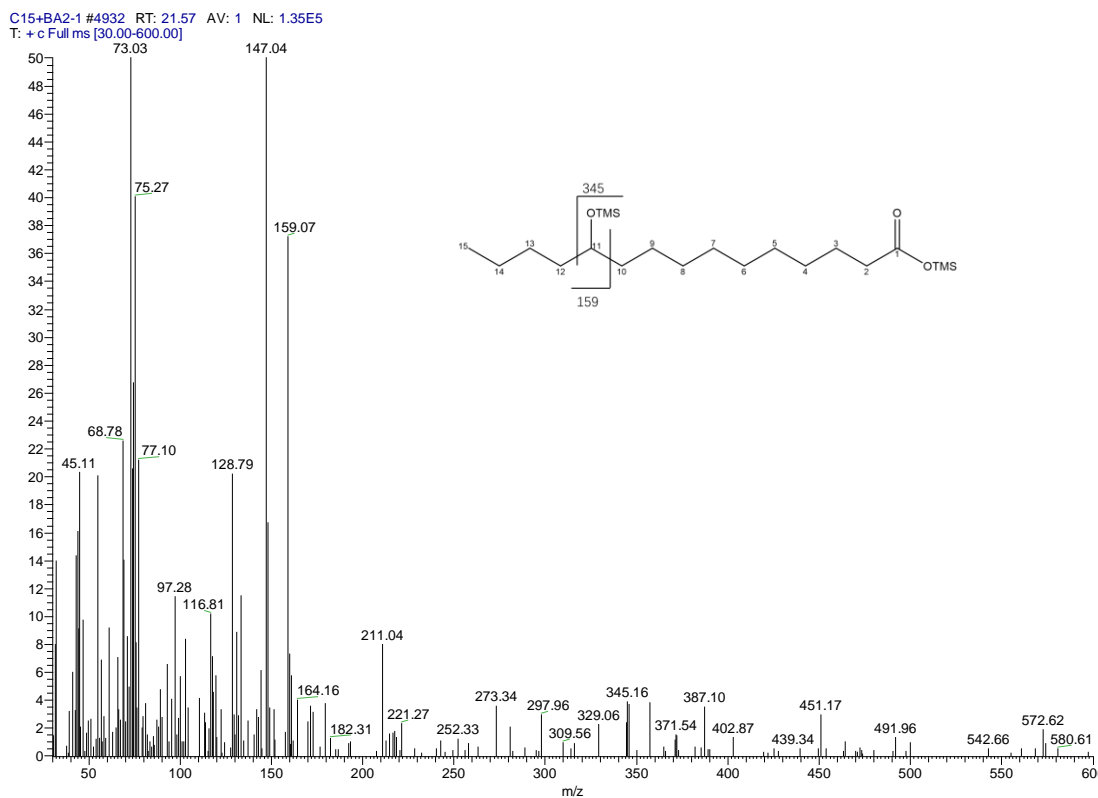
Tetradecanoic  $\omega$ -6, RT:17.89 min

Tetradecanoic  $\omega$ -7,

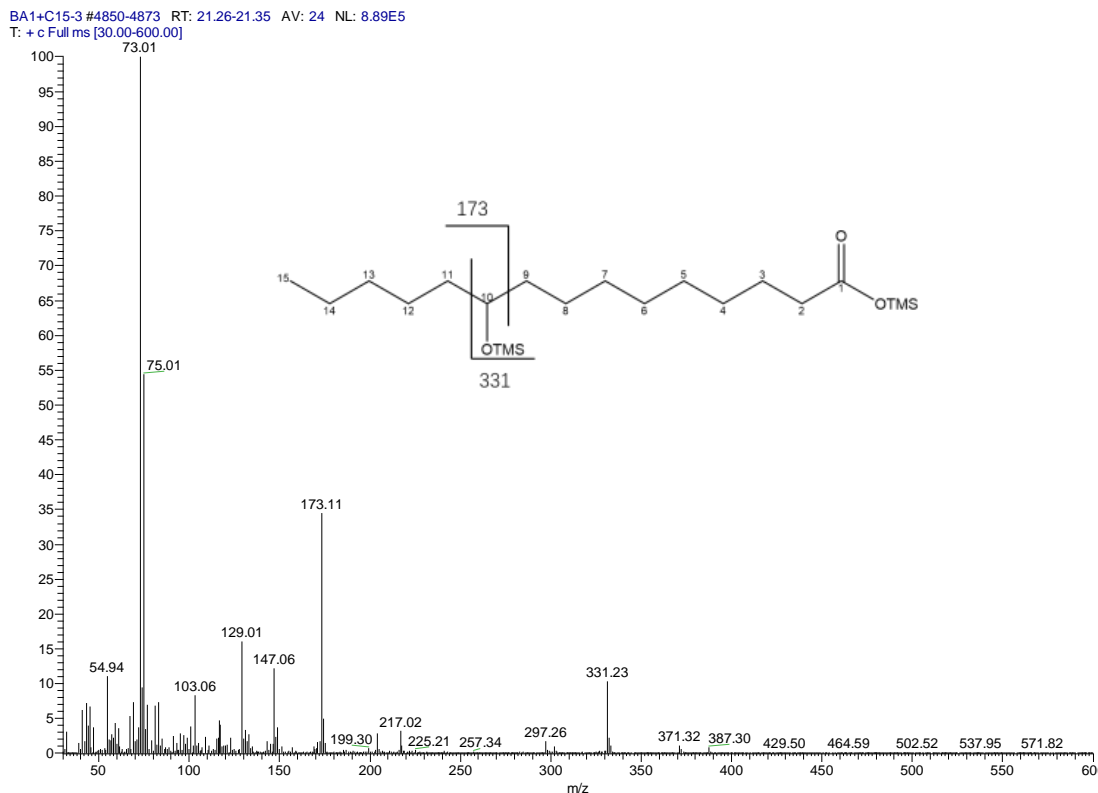
RT:17.74 min

Products from Pentadecanoic acid (C15:0)Pentadecanoic  $\omega$ -1, RT: 23.52 min

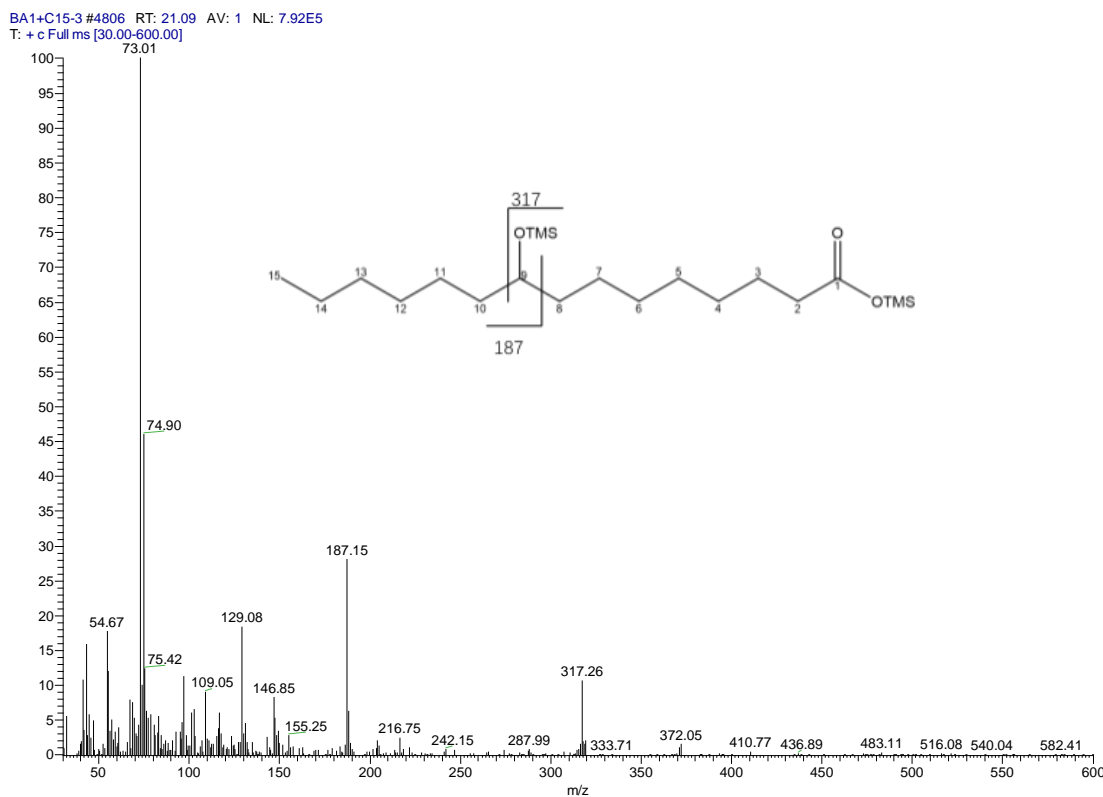
Pentadecanoic  $\omega$ -2, RT: 23.05 minPentadecanoic  $\omega$ -3, RT: 22.11 min



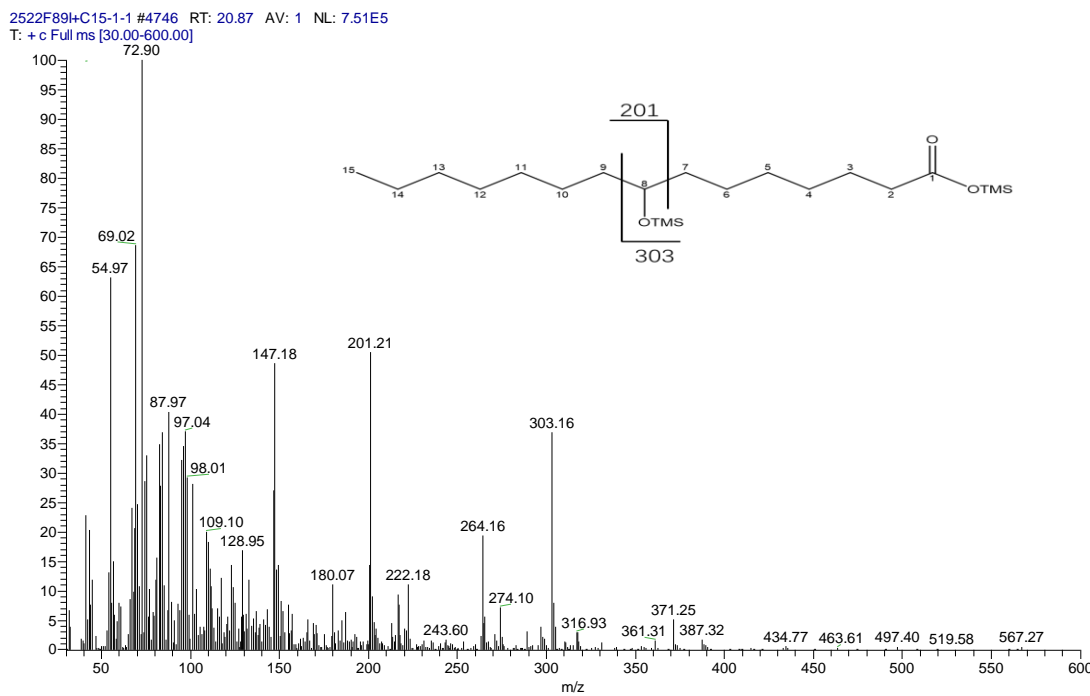
Pentadecanoic ω-4, RT: 21.58 min



Pentadecanoic ω-5, RT: 21.32min

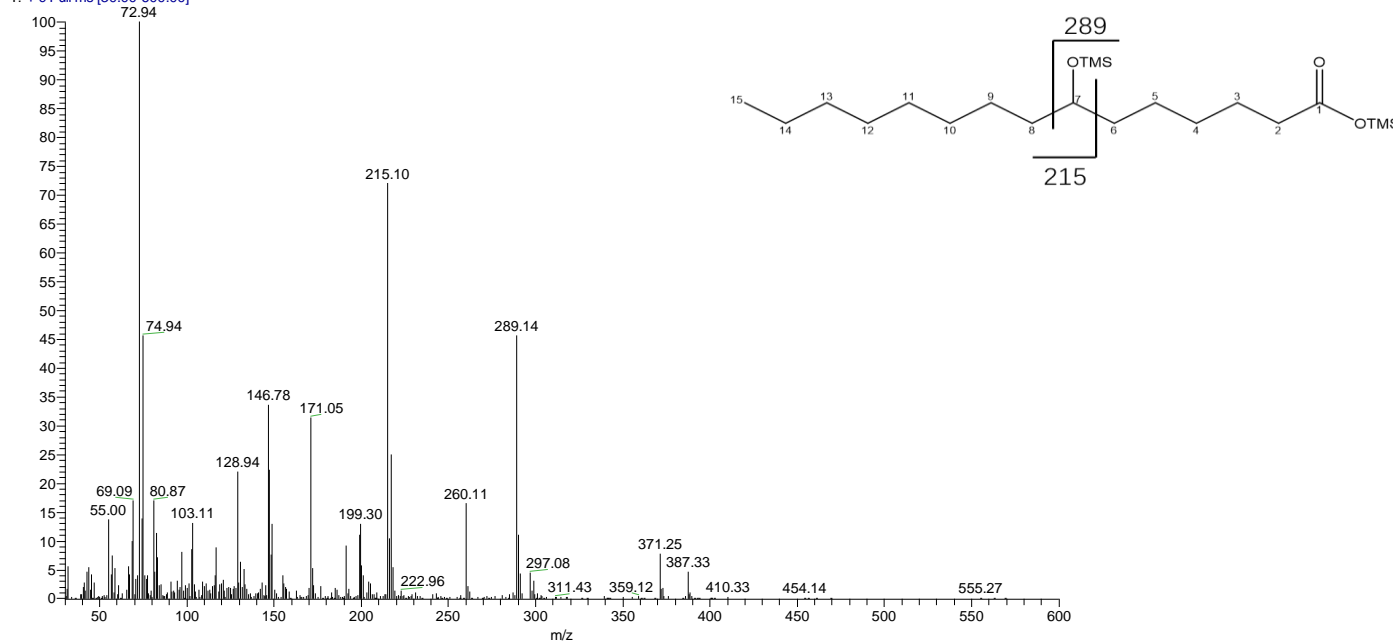


Pentadecanoic ω-6, RT: 21.00 min



Pentadecanoic ω-7, RT: 20.87 min

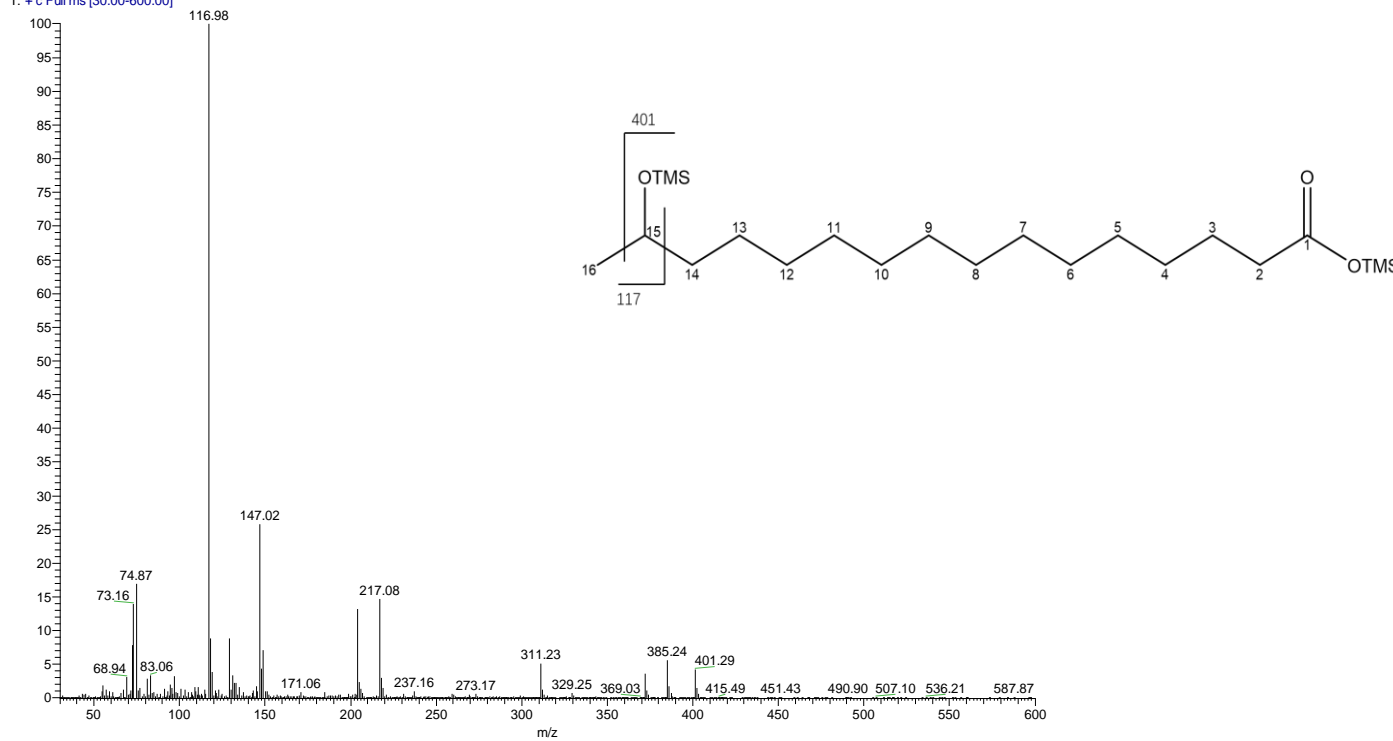
2522F89+H-C15-1-1 #4693 RT: 20.67 AV: 1 NL: 1.04E6  
T: + c Full ms [30.00-600.00]



Pentadecanoic  $\omega$ -8, RT: 20.67 min

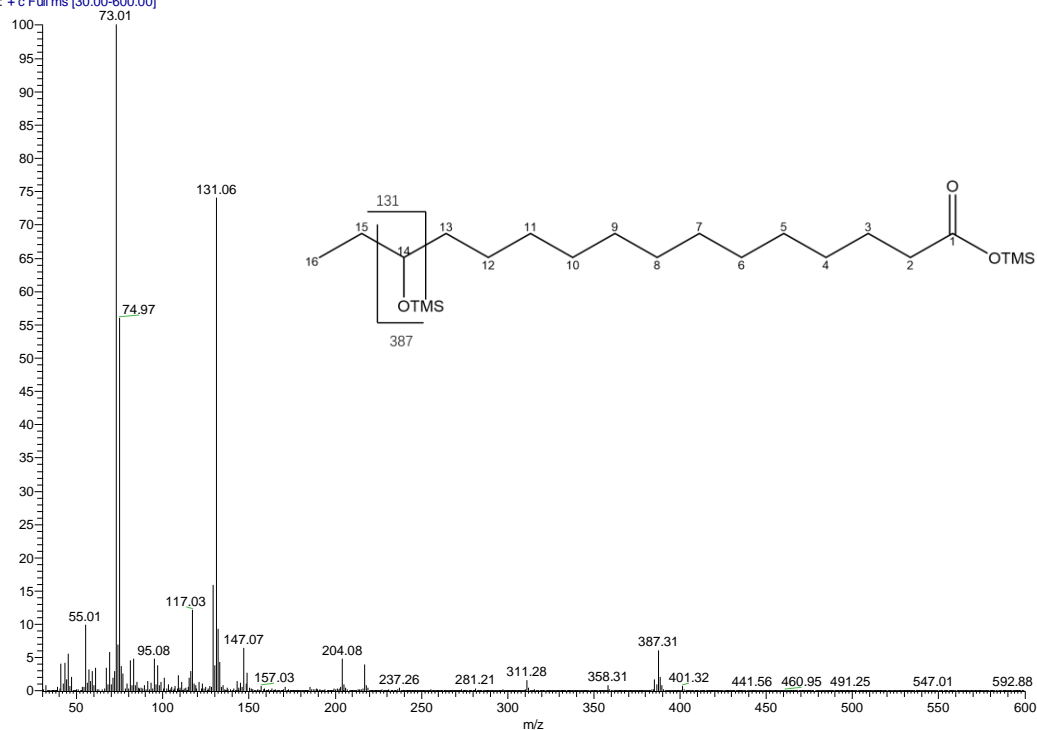
### Products from Palmitic acid (C16:0):

BA1-F89I-20H-1 #6430 RT: 27.28 AV: 1 NL: 4.57E7  
T: + c Full ms [30.00-600.00]



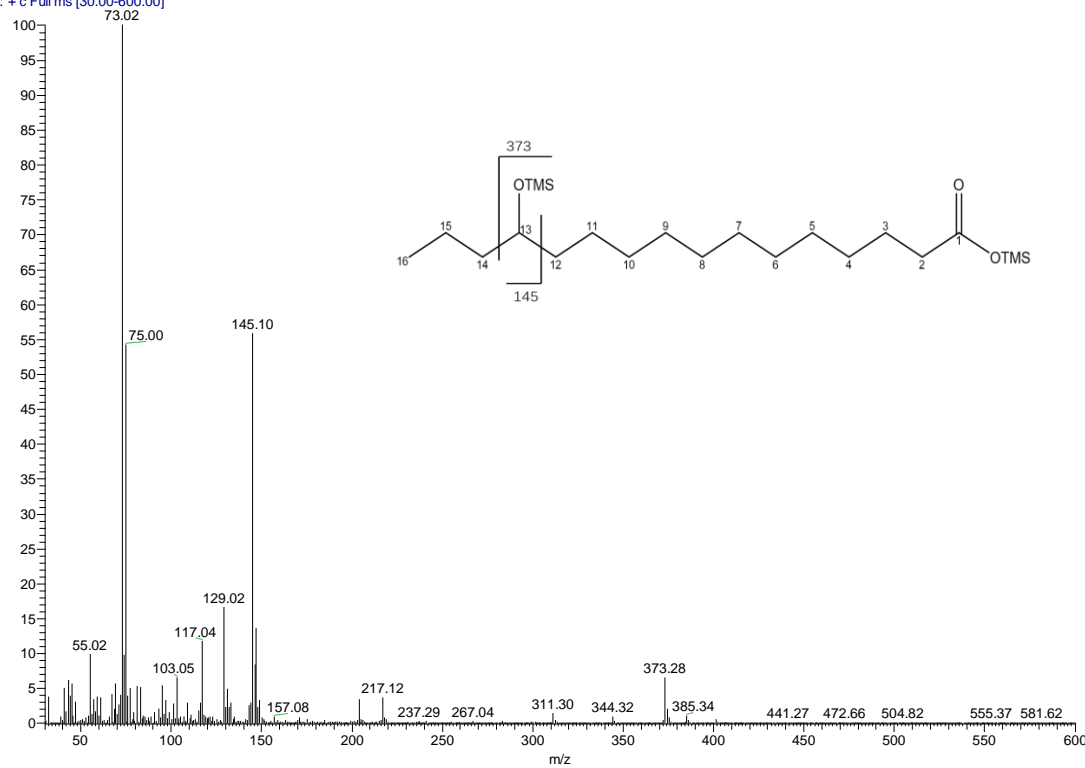
Palmitic  $\omega$ -1, RT: 27.05 min

c16+BA2-2 #6229-6267 RT: 26.45-26.60 AV: 39 NL: 3.93E6  
T: + c Full ms [30.00-600.00]



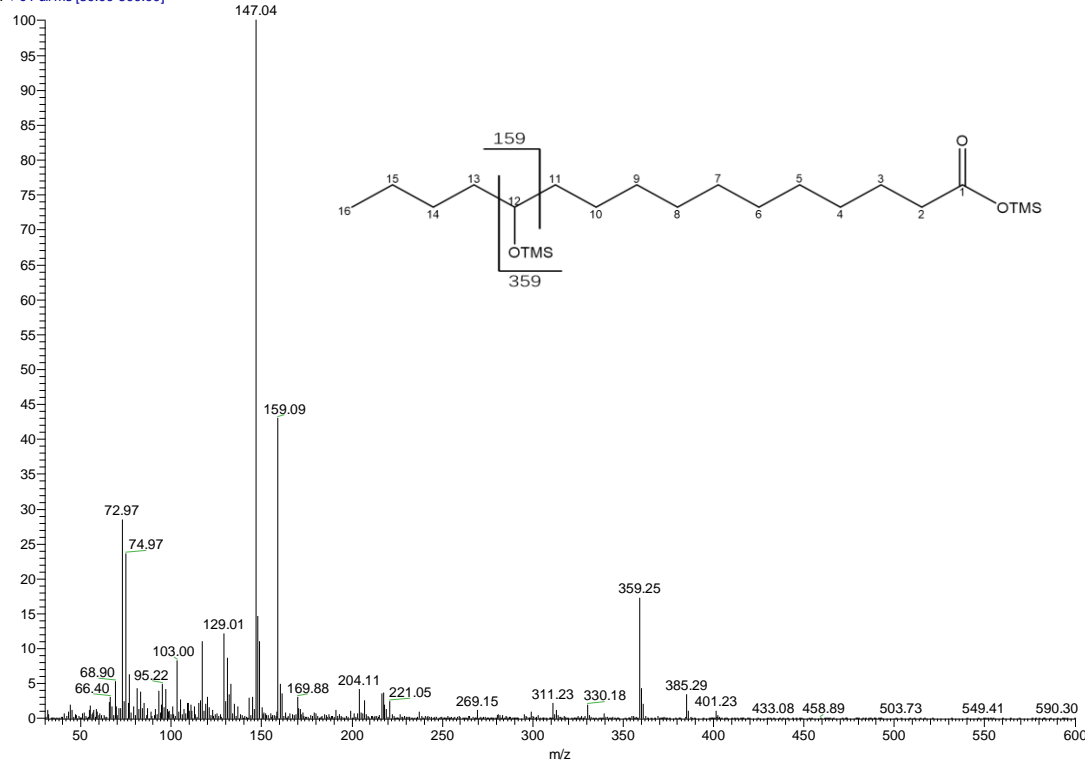
Palmitic  $\omega$ -2, RT: 26.57 min

c16+BA2-2 #5975-6013 RT: 25.50-25.64 AV: 39 NL: 9.06E5  
T: + c Full ms [30.00-600.00]



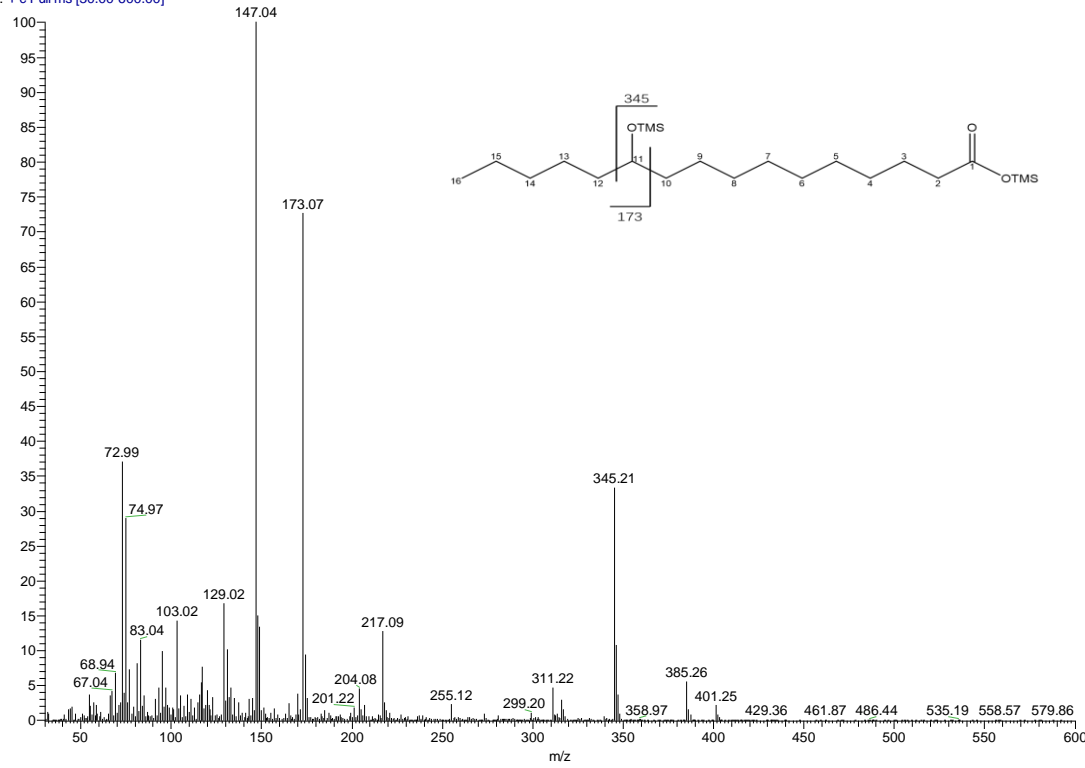
Palmitic  $\omega$ -3, RT: 25.57 min

BA1-F89I-20H-1 #5898 RT: 25.26 AV: 1 NL: 9.91E6  
T: + c Full ms [30.00-600.00]



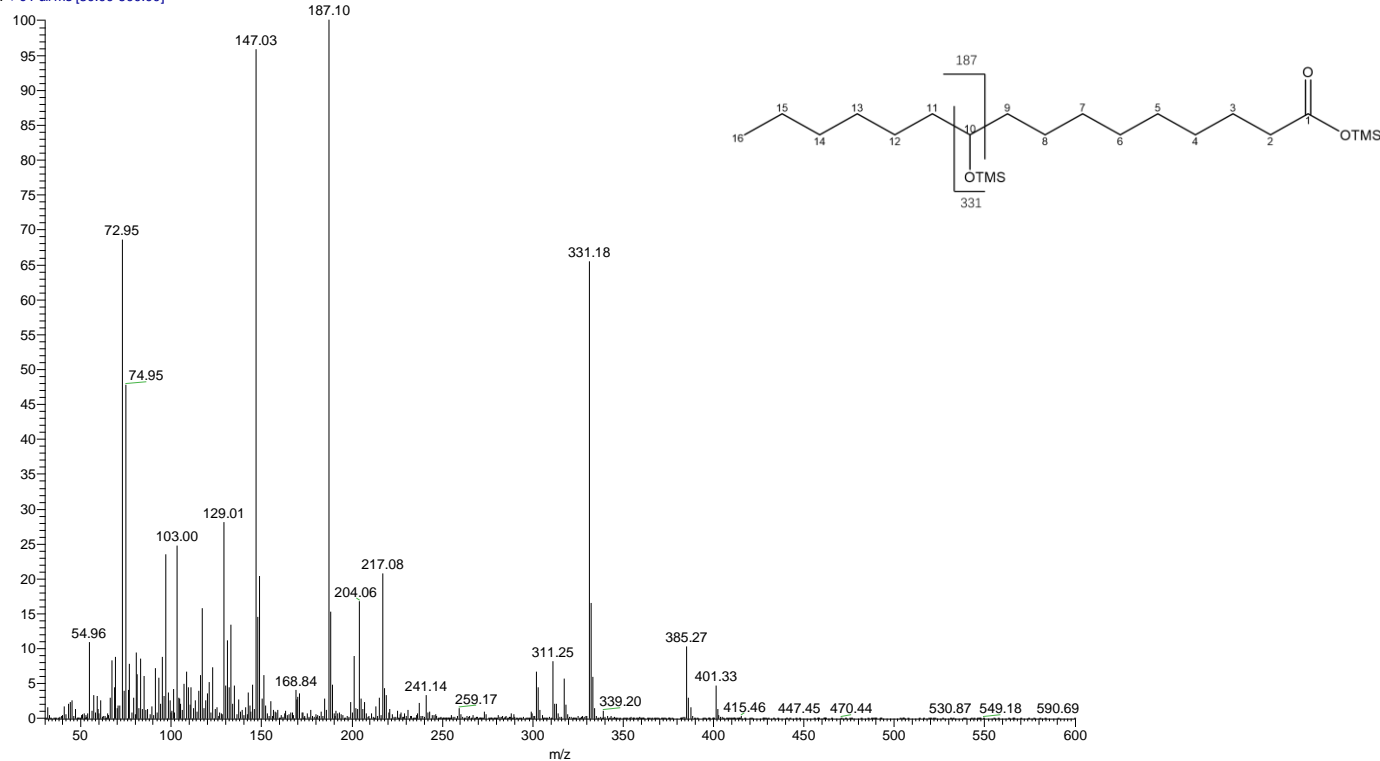
Palmitic  $\omega$ -4, RT: 25.26 min

BA1-F89I-20H-1 #5809 RT: 24.92 AV: 1 NL: 1.04E7  
T: + c Full ms [30.00-600.00]



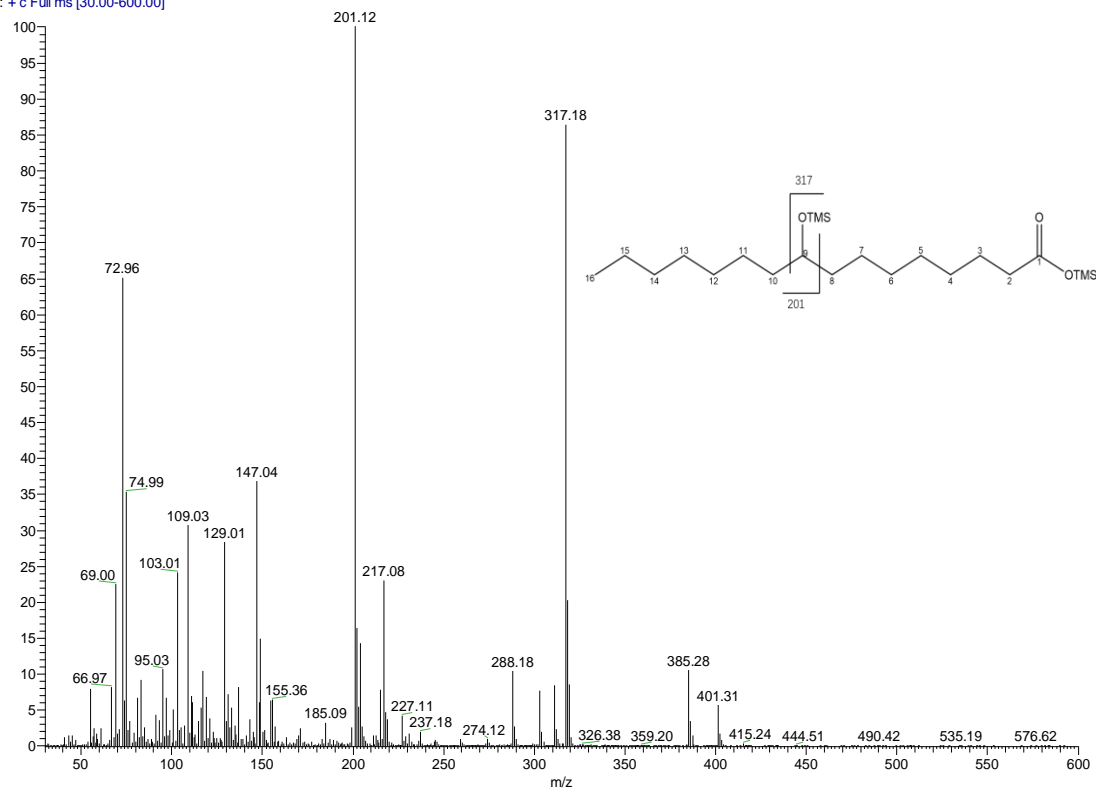
Palmitic  $\omega$ -5, RT: 24.92 min

BA1-F89I-20H-1 #5740 RT: 24.65 AV: 1 NL: 1.19E7  
T: + c Full ms [30.00-600.00]



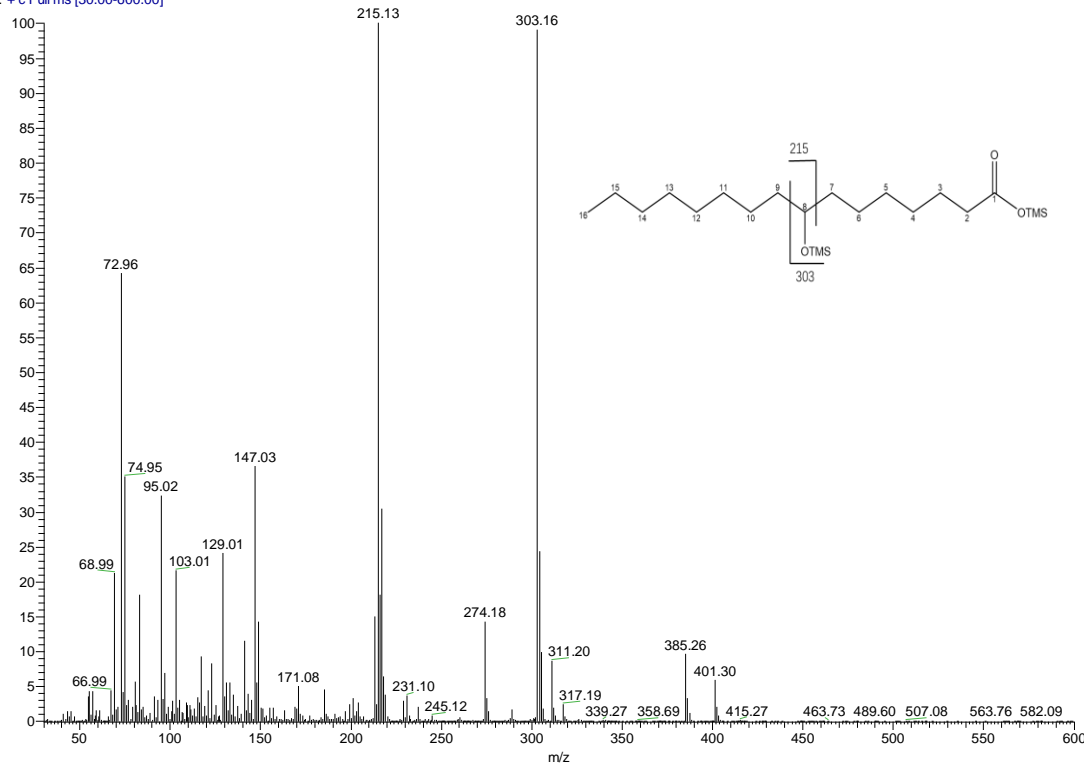
Palmitic  $\omega$ -6, RT: 24.92 min

BA1-F89I-20H-1 #5708 RT: 24.52 AV: 1 NL: 4.25E7  
T: + c Full ms [30.00-600.00]



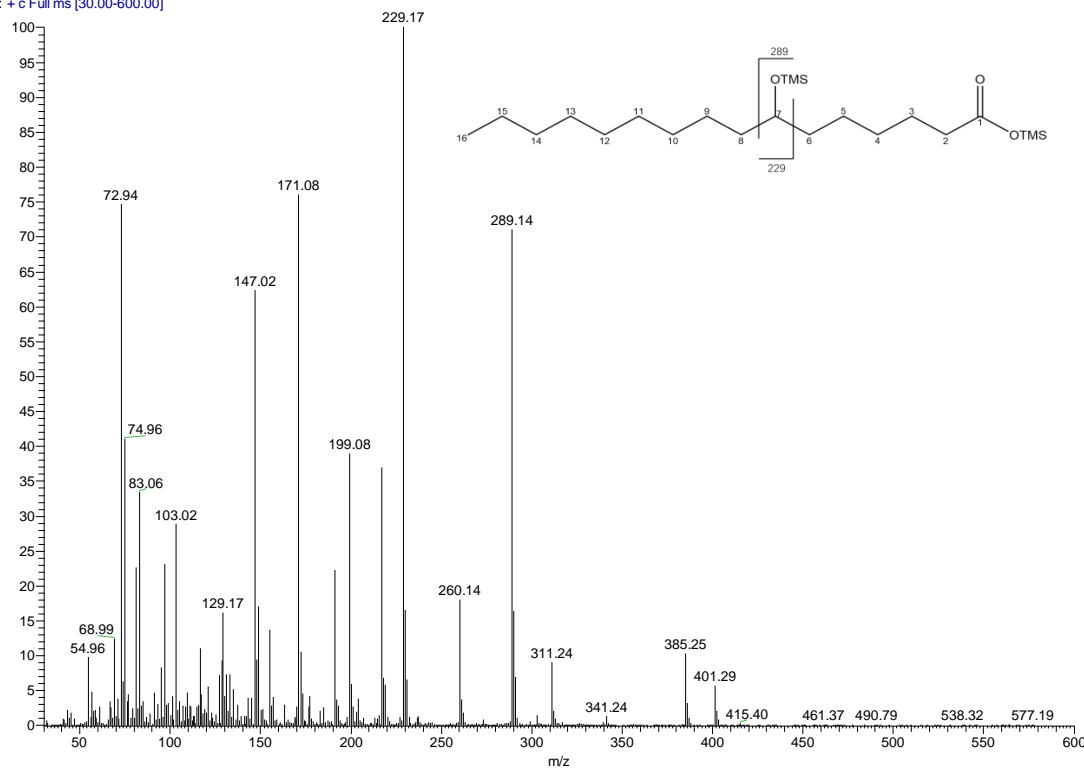
## Palmitic ω-7, RT: 24.52 min

BA1-F89I-20H-1 #5679 RT: 24.41 AV: 1 NL: 4.86E7  
T: + c Full ms [30.00-600.00]



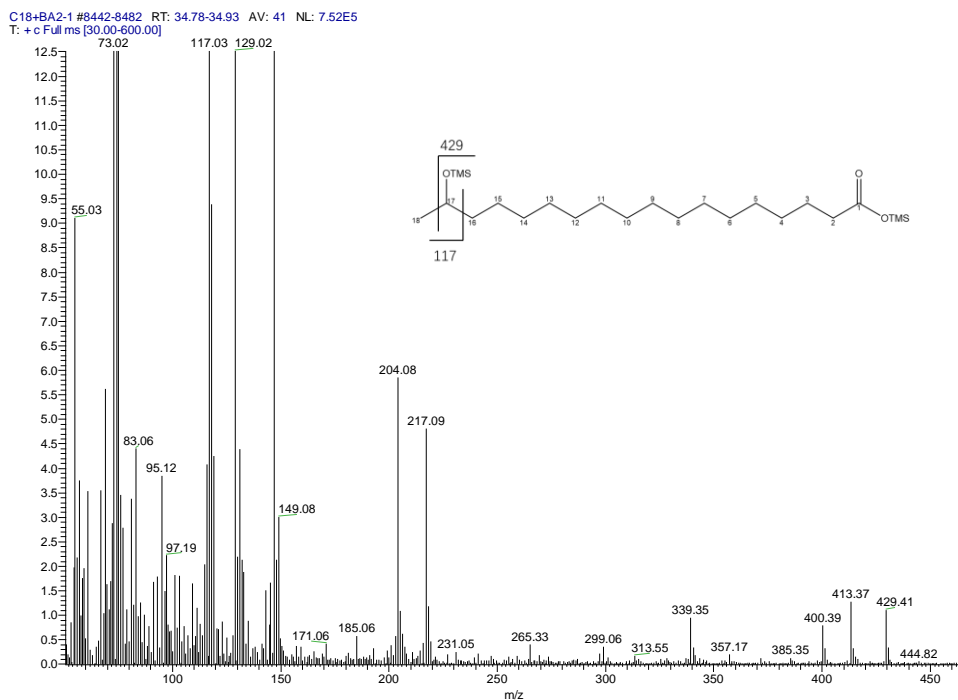
## Palmitic ω-8, RT: 24.41 min

BA1-F89I-20H-1 #5648 RT: 24.29 AV: 1 NL: 2.35E7  
T: + c Full ms [30.00-600.00]

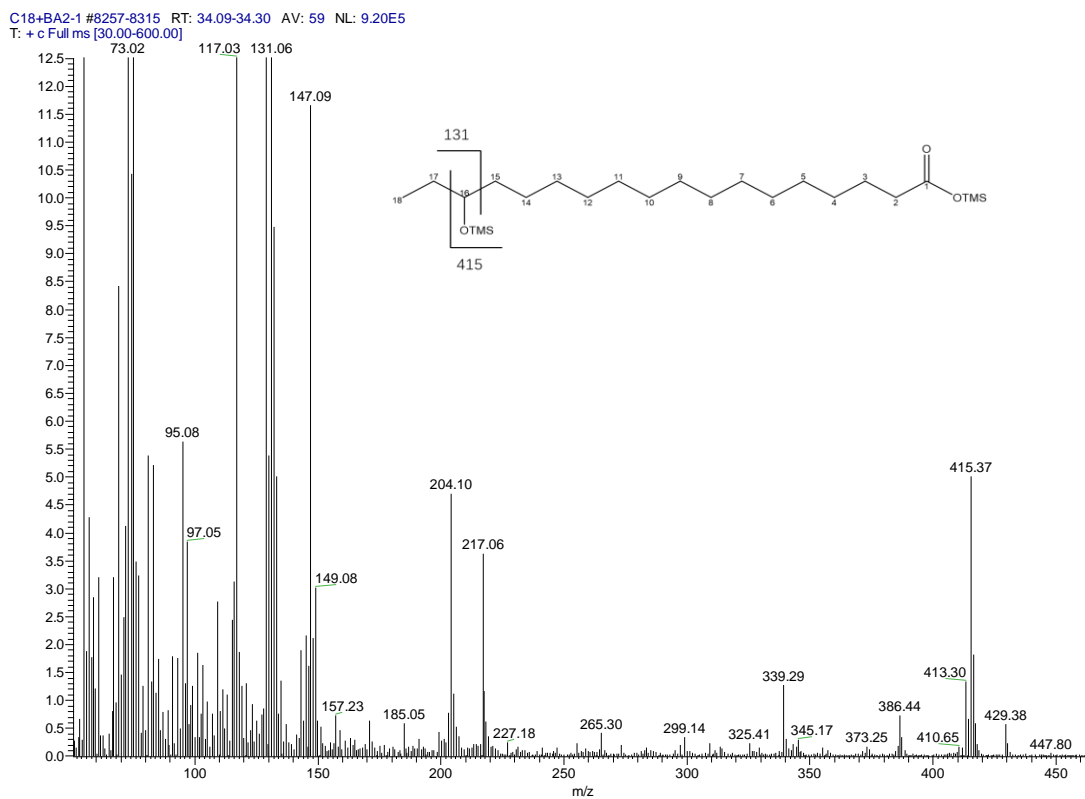


Palmitic ω-9, RT: 24.41 min.

**Products from Octadecanoic acid (C18:0):**

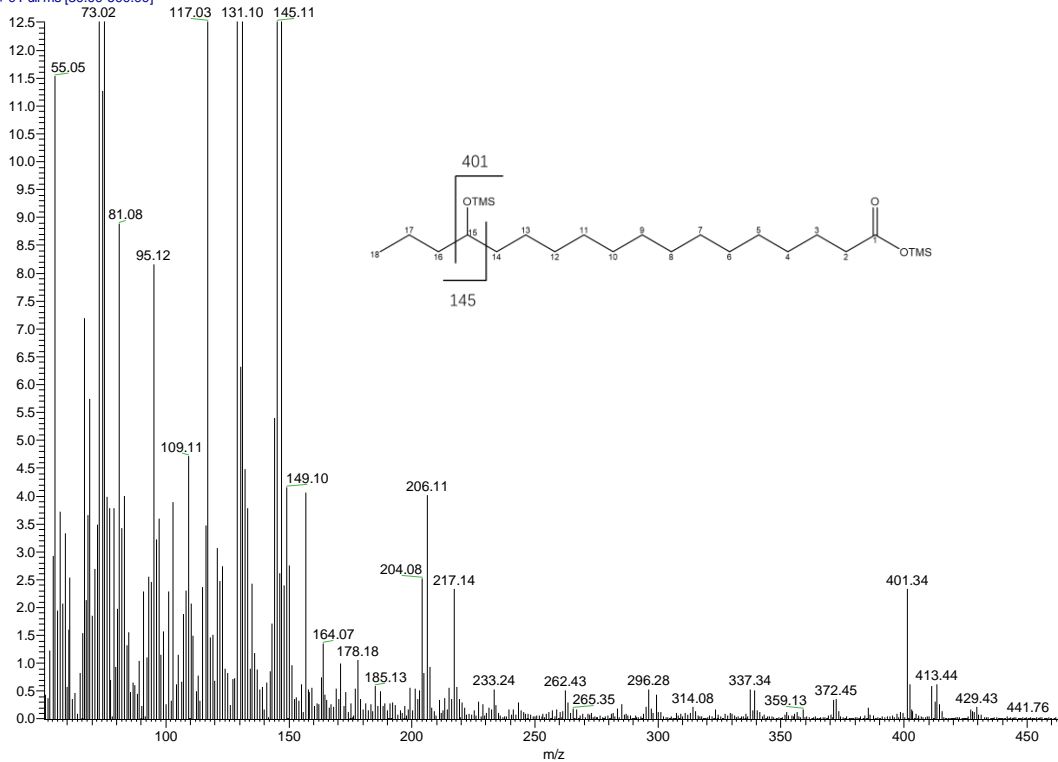


Octadecanoic ω-1, RT: 34.88 min



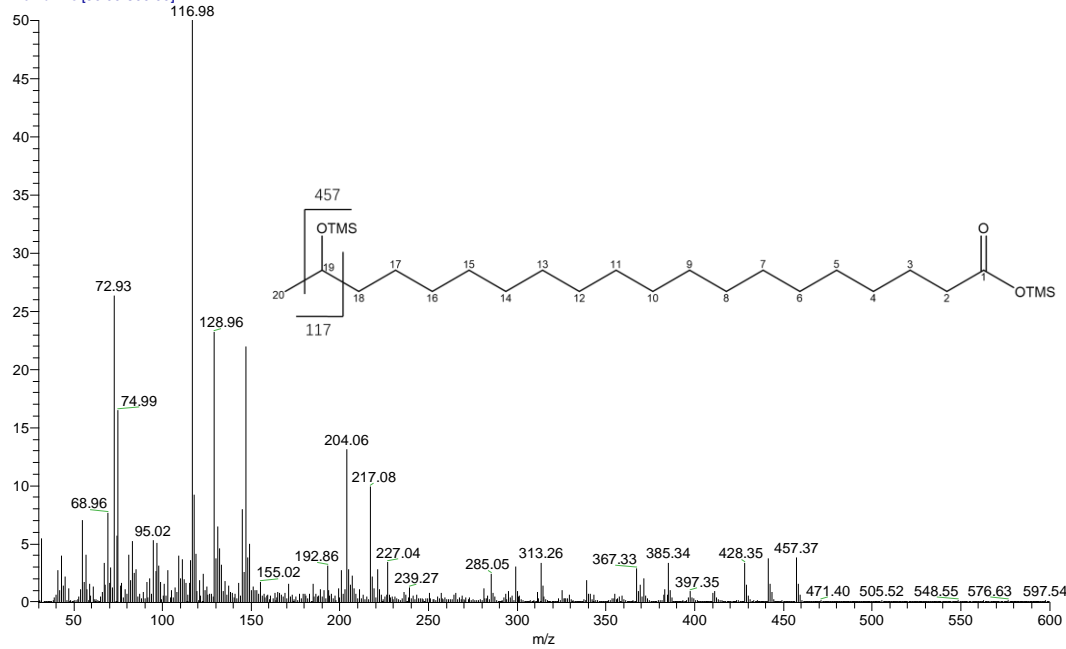
## Octadecanoic ω-2, RT: 34.23 min

C18+BA2-1 #7905-7968 RT: 32.76-33.00 AV: 64 NL: 7.72E5  
T: + c Full ms [30.00-600.00]



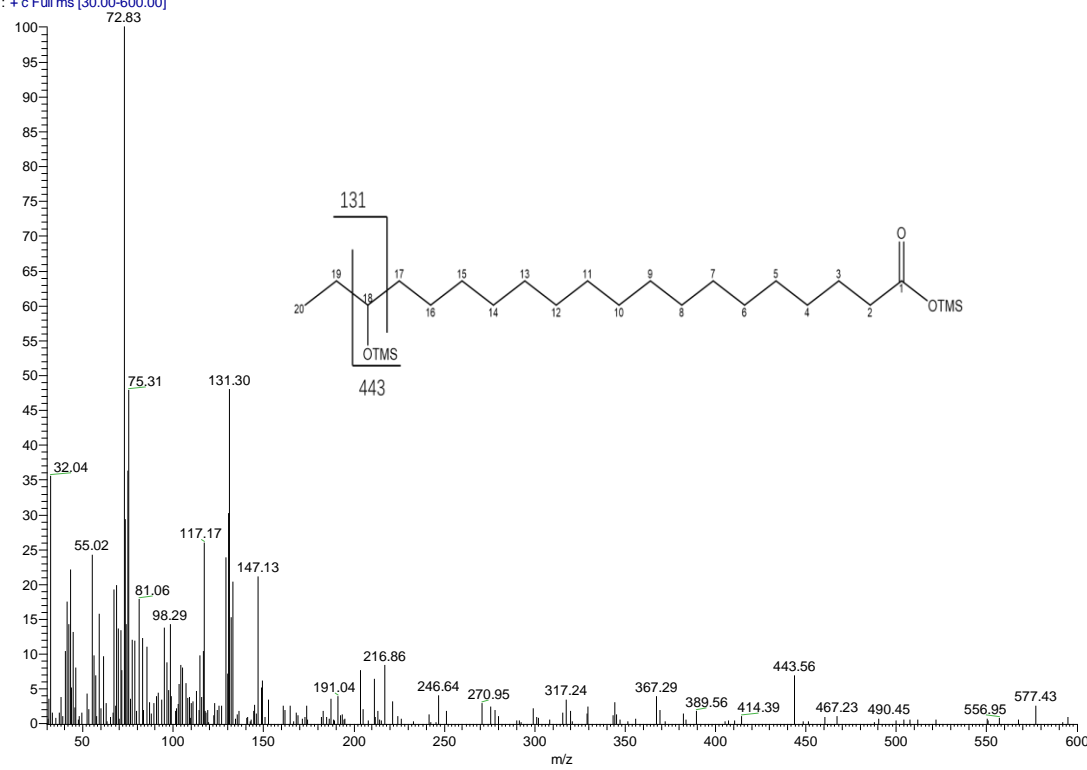
### Products from Arachidic acid (C20:0)

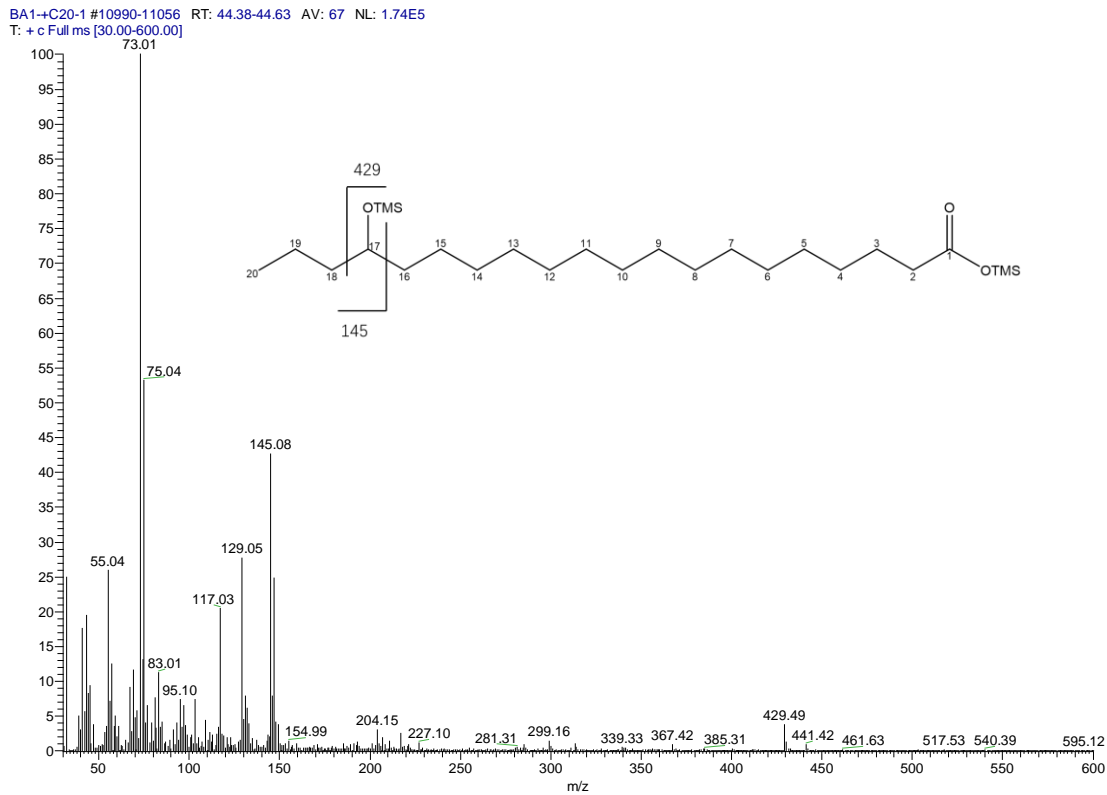
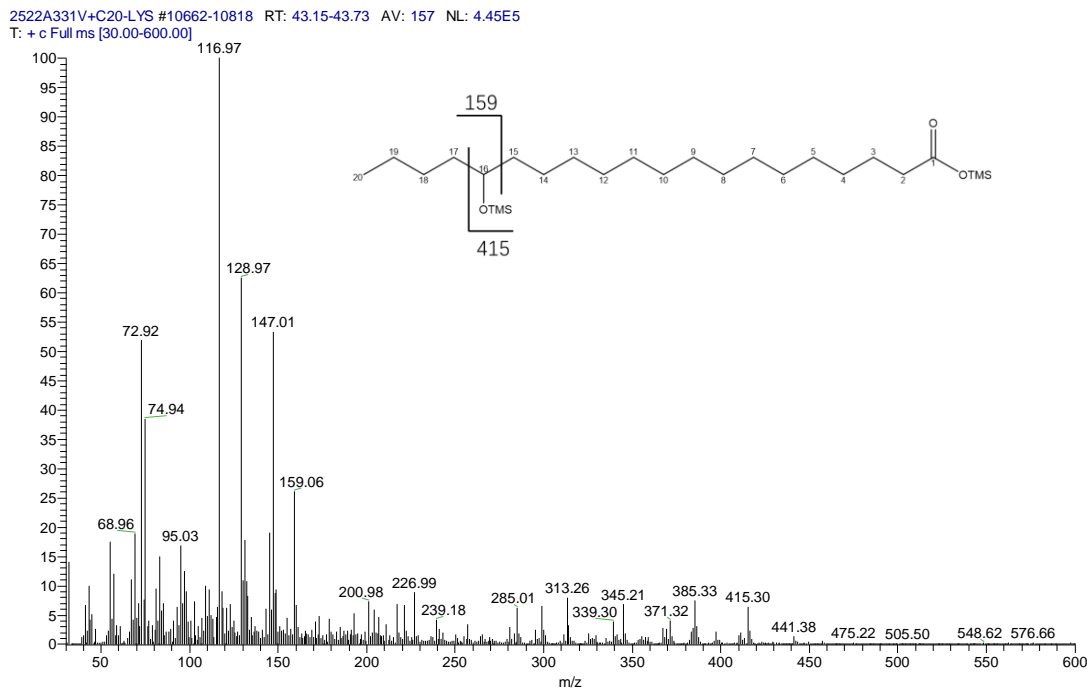
2522A331V+C20-bu #11860-11995 RT: 47.66-48.16 AV: 136 NL: 8.68E5  
T: + c Full ms [30.00-600.00]



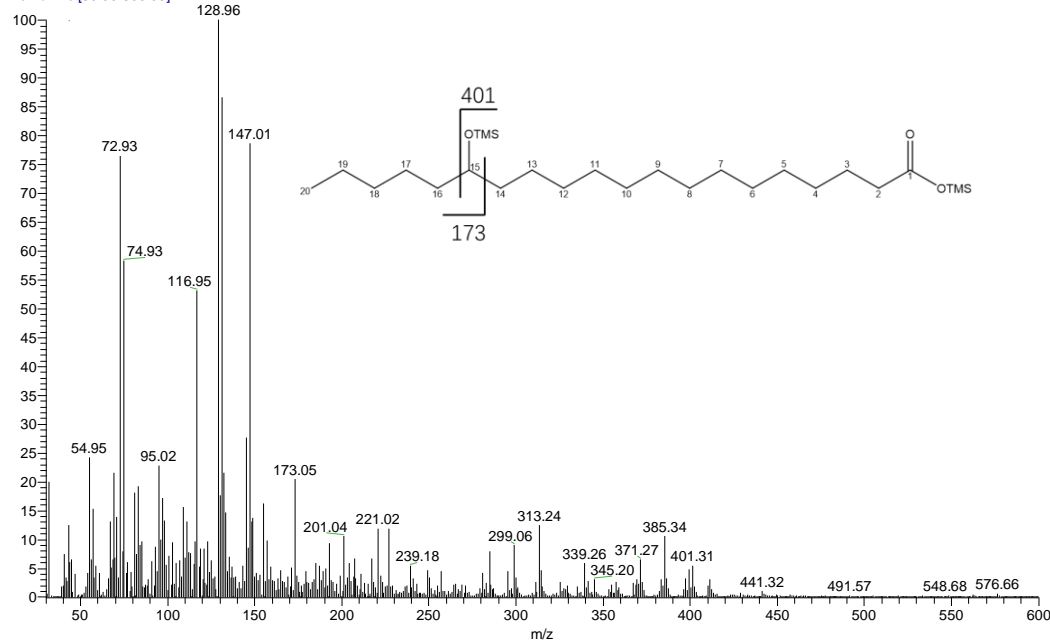
Arachidic  $\omega$ -1, RT: 47.91 min

BA1+C20-1 #11611 RT: 46.72 AV: 1 NL: 1.25E5  
T: + c Full ms [30.00-600.00]



Arachidic  $\omega$ -2, RT: 46.72 minArachidic  $\omega$ -3, RT: 44.50 minArachidic  $\omega$ -4, RT: 43.41 min

2522A331V+C20-LYS #10452-10570 RT: 42.35-42.80 AV: 119 NL: 3.14E5  
T: + c Full ms [30.00-600.00]



Arachidic ω-5, RT: 42.55 min